A NEW METHOD OF ESTIMATING WIND TUNNEL WALL INTERFERENCE IN THE UNSTEADY TWO-DIMENSIONAL FLOW

by

H. Sayada

National Aeronautical Establishment

86-02706/

NATIONAL AERONAUTICAL ESTABLISHMENT

SCIENTIFIC AND TECHNICAL PUBLICATIONS

AERONAUTICAL REPORTS:

Aeronautical Reports (LR): Scientific and technical information pertaining to aeronautics considered important, complete, and a lasting contribution to existing knowledge.

Mechanical Engineering Reports (MS): Scientific and technical information pertaining to investigations outside aeronautics considered important, complete, and a lasting contribution to existing knowledge.

AERONAUTICAL NOTES (AN): Information less broad in scope but nevertheless of importance as a contribution to existing knowledge.

LABORATORY TECHNICAL REPORTS (LTR): Information receiving limited distribution because of preliminary data, security classification, proprietary, or other reasons.

Details on the availability of these publications may be obtained from:

Publications Section,
National Research Council Canada,
National Aeronautical Establishment,
Bldg. M-16, Room 204,
Montreal Road,
Ottawa, Ontario
K1A 0R6

ÉTABLISSEMENT AÉRONAUTIQUE NATIONAL

PUBLICATIONS SCIENTIFIQUES ET TECHNIQUES

RAPPORTS D'AÉRONAUTIQUE

Rapports d'aéronautique (LR): Informations scientifiques et techniques touchant l'aéronautique jugées importantes, complètes et durables en termes de contribution aux connaissances actuelles.

Rapports de génie mécanique (MS). Informations scientifiques et techniques sur la recherche externe à l'aéronautique jugées importantes, complètes et durables en termes de contribution aux connaissances actuelles.

CAHIERS D'AÉRONAUTIQUE (AN): Informations de moindre portée mais importantes en termes d'accroissement des connaissances.

RAPPORTS TECHNIQUES DE LABORATOIRE (LTR): Informations peu disséminées pour des raisons d'usage secret, de droit de propriété ou autres ou parce qu'elles constituent des données préliminaires.

Les publications ci-dessus peuvent être obtenues à l'adresse suivante:

Section des publications
Conseil national de recherches Canada
Établissement aéronautique national
Im. M-16, pièce 204
Chemin de Montréal
Ottawa (Ontario)
K1A 0R6

UNLIMITED
UNCLASSIFIED

A NEW METHOD OF ESTIMATING WIND TUNNEL WALL INTERFERENCE IN THE UNSTEADY TWO-DIMENSIONAL FLOW

NOUVELLE MÉTHODE D'ESTIMATION DE LA PERTURBATION DES ÉCOULEMENTS INSTATIONNAIRES PAR LES PAROIS D'UNE SOUFFLERIE

by/par

H. Sawada, visiting scientist
2nd Aerodynamics Division,
National Aerospace Laboratory,
Japan

OTTAWA
JANUARY 1983

AERONAUTICAL NOTE
NAE-AN-9
NRC NO. 21274

L.H. Ohman, Head/Chef
High Speed Aerodynamics Laboratory/
Laboratoire d'aérodynamique à hautes vitesses

G.M. Lindberg
Director/Directeur

ABSTRACT

A new method of estimating wall interference in unsteady flow is presented. This method is valid for subcritical flow within the accuracy of the linearized small disturbance theory. The main feature of the method is the use of measured pressure along lines in the flow direction near the tunnel walls. This method is particularly effective in a tunnel with ventilated walls because it does not require the representation of wall characteristics with unreliable mathematical expressions. Results of some numerical examples indicate that the new method produces satisfactory results except for cases when the reduced frequencies are close to the tunnel resonance frequencies. For the case of an airfoil in pitching motion, the method has been used to correct the amplitude of the angle of attack and the time lag in the motion.

RÉSUMÉ

Une nouvelle méthode d'estimation de la perturbation des écoulements instationnaires par des parois est présentée. Elle s'applique aux écoulements subcritiques dans l'intervalle de précision permis par la théorie des petites perturbations linéarisées. Sa principale caractéristique est l'emploi de mesures de la pression tangentielle à l'écoulement près des parois de la soufflerie. La méthode est particulièrement utile dans les souffleries à parois ventilées car elle ne nécessite aucune représentation mathématique, souvent erronée, des caractéristiques des parois. Les résultats de quelques exemples numériques montrent que la nouvelle méthode donne des résultats satisfaisants, sauf lorsque les fréquences réduites approchent les fréquences de résonnance de la soufflerie. Pour un profil aérodynamique en tangage, la méthode a permis de corriger l'angle d'attaque et le retard dans le mouvement.

CONTENTS

		Page
SUMMARY		(iii)
NOTATIONS		(vi)
1. INTRODUCTION		1
2. ANALYSIS		1
3. SOME EXAMPLES OF CORRECTION		12
4. CONCLUSIONS		13
5. REFERENCES		14
APPENDIX A	Derivation of Equation (19)	45
APPENDIX B	Derivation of Equation (51)	51

ILLUSTRATIONS

Figure		Page
1	An Airfoil in Pitching Motion in Free Air	15
2	An Airfoil in Pitching Motion in a Tunnel	16
3	ΔK vs $\hat{x}/c$	17
4	WA vs $\hat{x}/c$	18
5	WA vs $\hat{x}/c$	19
6	WA vs $\hat{x}/c$	20
7	WA vs $\hat{x}/c$	21
8	WA vs $\hat{x}/c$	22
9	$\lvert C_L \rvert_\alpha$ vs $\hat{k}$	23
10	$\lvert \phi_L \rvert_\alpha$ vs $\hat{k}$	24
11	$\Delta\alpha_A$ vs $\hat{k}$	25
12	$\omega\Delta\tau$ vs $\hat{k}$	26
13	ΔC_p vs $\hat{x}/c$	27

ILLUSTRATIONS (Cont'd)

Figure		Page
14	ΔC_p vs $\hat{x}/c$	28
15	C_L vs α	29
16	C_L vs α	30
17	C_m vs α	31
18	C_m vs α	32
19	$\lvert C_L \rvert_\alpha$ vs $\hat{k}$	33
20	$\lvert \phi_L \rvert_\alpha$ vs $\hat{k}$	34
21	$\Delta\alpha_A$ vs $\hat{k}$	35
22	$\omega\Delta\tau$ vs $\hat{k}$	36
23	ΔC_p vs $\hat{x}/c$	37
24	ΔC_p vs $\hat{x}/c$	38
25	C_L vs α	39
26	C_L vs α	40
27	C_m vs α	41
28	C_m vs α	42
29	Domain of Flow Field in a Tunnel	43

NOTATIONS

Notations	Definition
a_∞	sound speed of undisturbed uniform flow
C_p	pressure coefficient
$\tilde{C}_{p0}, \tilde{C}_{pc}, \tilde{C}_{ps}$	defined in Equation (22)
C_{pH}	pressure coefficient at z = H
$C_{p0}^H, C_{pc}^H, C_{ps}^H$	Equation (56)
CH	Equation (57)
C_L	lift coefficient
C_{Lc}, C_{Ls}	defined in Equation (92)
$\lvert C_L \rvert_\alpha$	$\lvert C_L \rvert$ due to unit pitching motion
$\tilde{C}_p$	defined in Equation (27)
$\tilde{CP}$	defined in Equation (21)
CP	defined in Equation (53)
c	airfoil chord length
f_c, f_s	defined in Equation (78)
H	$= \beta \hat{H}$
$\hat{H}$	tunnel semi-height
H_0	the Struve function
$h_A, \tilde{h}_A$	amplitude of plunging motion
i	imaginary number
I	defined in Equation (74) or (85)
J_0	Bessel function
K	defined in Equation (59)
$\tilde{K}$	defined in Equation (34)
$\tilde{K}_r, \tilde{K}_i$	defined in Equations (36) and (37)

NOTATIONS (Cont'd)

Notations	Definition
k	an integer
$\hat{k}$	reduced frequency $= \frac{c\hat{\omega}}{2U_\infty}$
M	a large positive number
M_∞	uniform flow Mach number
m	an integer
n	normal outward co-ordinate to $\partial\Omega$ or an integer
N_0	the Newmann function, Equation (A-21)
P	defined in Equation (A-10)
Q	a large positive number
R	a large positive number
S_c	defined in Equation (80)
$\tilde{S}_c$	defined in Equation (83)
S_{c0}	mean camber of airfoil
t	transformed time variable, Equation (5)
$\hat{t}$	time
U_∞	uniform flow speed
w	upwash along the z-axis
w_c, w_s	defined in Equation (66)
$\tilde{w}_c, \tilde{w}_s$	defined in Equation (39)
WA	defined in Equation (60)
W_r, W_i	defined in Equations (63) and (64)
W	defined in Equation (65)
$\tilde{W}$	defined in Equation (38)
W_i	defined in Equation (73)
$\hat{x}$	distance measured from the pitch axis in the uniform flow direction

NOTATIONS (Cont'd)

Notations	Definition
x	transformed $\hat{x}$, Equation (5)
$\hat{x}_L$	leading edge $\hat{x}$-co-ordinate
$\hat{x}_T$	trailing edge $\hat{x}$-co-ordinate
x_L, x_T	transformed $\hat{x}_L$ and $\hat{x}_T$
$\hat{z}$	distance upward from $\hat{x}$-axis
z	transformed z, Equation (5)
$\alpha, \tilde{\alpha}$	angle of attack
$\alpha_0, \tilde{\alpha}_0$	time-averaged angle of attack
$\alpha_A, \tilde{\alpha}_A$	amplitude of angle of attack of pitching motion
β	defined in Equation (4)
γ	Euler constant (=0.5772156649)
$\Delta C_{pc}, \Delta C_{ps}$	defined in Equation (53)
$\Delta\tilde{C}_{pc}, \Delta\tilde{C}_{pc}, \Delta\tilde{C}_{ps}$	defined in Equation (32)
$\Delta\tilde{C}_p$	pressure coefficient difference between the upper and lower airfoil surfaces
ΔCP	defined in Equation (71)
ΔK	defined in Equation (70)
$\Delta K_r, \Delta K_i$	defined in Equations (61) and (62)
ΔW	defined in Equation (69)
$\Delta\alpha_A$	$= \tilde{\alpha}_A - \alpha_A$
$\Delta\tau$	time lag of pitching motion, Equation (1)
$\partial\Omega$	boundary of Ω
$\partial\Omega_\rho$	a small circle with the radius ρ and the center at (x,z)
$\partial\Omega_R$	a big circle with the radius R and the center at (x,z)
ϵ	a small positive number
ϑ, θ	integral variables

NOTATIONS (Cont'd)

Notations	Definition
κ	defined in Equation (15)
(ξ, ζ)	(x,z)
ρ	a small positive number
$\hat{\Phi}; \tilde{\hat{\Phi}}$	full velocity potential functions
$\hat{\phi}, \tilde{\hat{\phi}}$	small perturbation velocity potential functions, Equations (42) and (43)
$\tilde{\hat{\phi}}_0, \tilde{\hat{\phi}}_c, \tilde{\hat{\phi}}_s$	defined in Equation (8)
$\tilde{\phi}_0, \tilde{\phi}_c, \tilde{\phi}_s$	defined in Equation (10)
ϕ	transformed $\hat{\phi}$, Equation (43)
ϕ^*	defined in Equation (45)
$\tilde{\phi}^*$	defined in Equation (14)
$\phi_{L\alpha}$	phase lag in lift, Equation (91)
ψ	analytical real valued function in Ω, Equation (47)
$\tilde{\psi}$	defined in Equation (17)
ψ	integral variable
Ω	a part of flow field
$\hat{\omega}$	angular velocity of pitching or plunging motion
ω	transformed $\hat{\omega}$, Equation (9)
O,o	the Landau's symbol, Equations (A-30) and (B-9)
sign (x)	$= \begin{matrix} 1 \text{ for } x > 0 \\ -1 \text{ for } x < 0 \end{matrix}$
$(\bar{\ })$	averaged value over the airfoil

A NEW METHOD OF ESTIMATING WIND TUNNEL WALL INTERFERENCE IN THE UNSTEADY TWO-DIMENSIONAL FLOW

1. INTRODUCTION

The unsteady wall interference problem has not been as thoroughly investigated as the steady case (Refs. 1 - 5). A new method of estimating the wall interference in unsteady subsonic flow is presented in this paper. The method requires the time-dependent pressure along lines in the flow direction near the tunnel walls and on the airfoil model to be measured. The pressure along the lines will be that on the walls if the tunnel walls are solid. This method is particularly effective if the walls are ventilated, since the method is valid no matter how complicated the wall characteristics may be. The merit of this approach is similar to that for steady flow which were developed by several researchers (Refs. 6 - 10). There is only a slight difference between the steady and unsteady wall interference problem, and that lies in the fundamental equation for the small perturbation potential. In incompressible flow, even this difference vanishes and the wall corrections can be obtained using similar method developed for steady flow. The new method will first be presented in the analytical way and then some examples of the corrections for a pitching airfoil will be calculated. The data used here are not obtained by tunnel tests but by numerical means.

2. ANALYSIS

Suppose a thin airfoil is in pitching motion with a constant angular velocity $\hat{\omega}$ in free air. In this case it is convenient to locate the origin of a space co-ordinate system $(\hat{x},\hat{z})$ at the pitch axis, where $\hat{x}$ is the distance measured from this axis along the uniform flow direction and $\hat{z}$ is the distance perpendicular to the $\hat{x}$ axis. The time $\Delta\tau$ is defined as the time when the time-dependent averaged positions of the airfoil coincide. The angle of attack, $\tilde{\alpha}$, (Fig. 1) for this airfoil can be written as follows:

$$\tilde{\alpha}(t) = \tilde{\alpha}_0 + \tilde{\alpha}_A \cdot \sin\{\hat{\omega}(\hat{t} - \Delta\tau)\} . \tag{1}$$

In order to simplify the analysis, the flow is assumed to be inviscid, irrotational and subcritical everywhere. Furthermore the thin airfoil approximation is also assumed to be valid. By the aid of these assumptions, the fundamental equation for the small disturbance potential function $\tilde{\hat{\phi}}$ can be written as

$$(1-M_\infty^2)\cdot\tilde{\hat{\phi}}_{\hat{x}\hat{x}} + \tilde{\hat{\phi}}_{\hat{z}\hat{z}} - 2\cdot\frac{M_\infty}{a_\infty}\cdot\tilde{\hat{\phi}}_{\hat{x}\hat{t}} - \frac{1}{a_\infty^2}\cdot\tilde{\hat{\phi}}_{\hat{t}\hat{t}} = 0 , \tag{2}$$

where $\tilde{\hat{\phi}}$ is defined as follows:

$$\tilde{\hat{\Phi}} = U_\infty\cdot\hat{x} + \tilde{\hat{\phi}} . \tag{3}$$

$\tilde{\phi}(x,z)$ is the full velocity potential function. M_∞ and a_∞ are the Mach number and the sonic speed for the undisturbed flow infinite upstream. Variables are introduced as follows:

$$\beta^2\cdot\tilde{\hat{\phi}} = c\cdot U_\infty\cdot\tilde{\phi} , \quad \beta = \sqrt{1-M_\infty^2} , \tag{4}$$

$$\text{and} \quad (\hat{x},\hat{z},\hat{t}) = \left(c\cdot x, \frac{c}{\beta}\cdot z, \frac{c}{a_\infty}\cdot\frac{1}{\beta}\cdot t\right), \tag{5}$$

where c is the chord length of the airfoil. Equation (2) becomes

$$\nabla^2\hat{\phi} - 2\cdot\frac{M_\infty}{\beta}\cdot\hat{\phi}_{xt} - \hat{\phi}_{tt} = 0 , \tag{6}$$

where the operator ∇^2 is

$$\nabla^2 \equiv \frac{\partial^2}{\partial x^2} + \frac{\partial^2}{\partial z^2} . \tag{7}$$

Suppose the flow disturbed by the oscillating airfoil with constant angular velocity $\hat{\omega}$ is also periodical in time with the same angular velocity everywhere, within the accuracy of the small disturbance theory, then $\tilde{\hat{\phi}}$ can be written

$$\tilde{\hat{\phi}}(\hat{x},\hat{z}) = \tilde{\hat{\phi}}_0(\hat{x},\hat{z}) + \tilde{\hat{\phi}}_s(\hat{x},\hat{z})\cdot\sin(\hat{\omega}\cdot\hat{t}) + \tilde{\hat{\phi}}_c(\hat{x},\hat{z})\cdot\cos(\hat{\omega}\cdot\hat{t}) . \tag{8}$$

Defining ω as

$$\omega = \frac{c}{a_\infty}\cdot\frac{1}{\beta}\cdot\hat{\omega} , \tag{9}$$

gives

$$\tilde{\phi}(x,z) = \tilde{\phi}_0(x,z) + \tilde{\phi}_s(x,z)\cdot\sin(\omega\cdot t) + \tilde{\phi}_c(x,z)\cdot\cos(\omega\cdot t) , \tag{10}$$

where $\tilde{\phi}_0$, $\tilde{\phi}_c$ and $\tilde{\phi}_s$ correspond to ϕ_0, ϕ_c and ϕ_s in Equation (4).

Substituting Equation (10) for $\tilde{\phi}$ into Equation (6) gives

$$\nabla^2\tilde{\phi}_0 = 0 , \tag{11}$$

$$\nabla^2\tilde{\phi}_c - 2\cdot\frac{\omega M_\infty}{\beta}\cdot\tilde{\phi}_{sx} + \omega^2\cdot\tilde{\phi}_c = 0 , \tag{12}$$

and

$$\nabla^2\tilde{\phi}_s + 2\cdot\frac{\omega M_\infty}{\beta}\cdot\tilde{\phi}_{cx} + \omega^2\cdot\tilde{\phi}_s = 0 . \tag{12a}$$

Introducing the new function ϕ^* defined as

$$\tilde{\phi}^* = (\tilde{\phi}_c + i\,\tilde{\phi}_s)\cdot e^{i\frac{\omega M_\infty}{\beta}\cdot x} . \tag{13}$$

Equations (12) and (12a) can be combined into one equation:

$$\nabla^2\tilde{\phi}^* + \kappa^2\cdot\tilde{\phi}^* = 0 , \tag{14}$$

where

$$\kappa = \omega/\beta . \tag{15}$$

From Green's theorem, the following expression for $\tilde{\phi}^*$ can be obtained:

$$\iint_{\Omega} (\tilde{\phi}^* \cdot \nabla^2 \tilde{\psi} - \tilde{\psi} \cdot \nabla^2 \tilde{\phi}^*) \, d\Omega = \oint_{\partial\Omega} (\tilde{\phi}^* \cdot \frac{\partial \psi}{\partial n} - \psi \cdot \frac{\partial \tilde{\phi}^*}{\partial n}) \, ds \quad , \tag{16}$$

where $\tilde{\psi}$ is a real valued analytical function throughout the flow field Ω and $\partial\Omega$ is its boundary and n is the outward normal co-ordinate to $\partial\Omega$. The following form for ψ is considered here:

$$\tilde{\psi}(\xi,\zeta;x,z) = \frac{1}{2\pi} \int_0^1 \frac{1}{\sqrt{1-\theta^2}} \cdot \sin\{\kappa|\zeta - z|\sqrt{1-\theta^2}\} \cdot \cos\{\kappa(\xi - x)\theta\} \, d\theta$$

$$- \frac{1}{2\pi} \int_1^{\infty} \frac{1}{\sqrt{\theta^2-1}} \cdot e^{-\kappa|\zeta - z|\sqrt{\theta^2-1}} \cdot \cos\{\kappa(\xi - x)\theta\} \, d\theta \, . \tag{17}$$

$\tilde{\psi}$ is continuous and differentiable two times with ξ and ζ except the point (x,z) and satisfies the following equation except at that point:

$$\nabla^2 \tilde{\psi} + \kappa^2 \cdot \tilde{\psi} = 0 \, . \tag{18}$$

Define Ω as the full space except the point (x,z) and the x axis downstream from the leading edge, Equation (16) reduces to the following expression:

$$\tilde{\phi}^*(x,z) = - \int_{x_L}^{\infty} [\tilde{\phi}^*]_-^+ \cdot \frac{\partial \tilde{\psi}}{\partial \zeta}\Big|_{\zeta=0} d\xi \, , \tag{19}$$

where

$$[\phi]_-^+ = \lim_{\zeta \to 0+} \{\phi(\xi,\zeta) - \phi(\xi,-\zeta)\} \, . \tag{20}$$

Appendix A can be referred to for the detailed derivation of the above equation. x_L is the point which corresponds to the leading edge $\hat{x}$-co-ordinate $\hat{x}_L$ in Equation (5).

The dynamic pressure coefficient $\tilde{C}_p(x,z,t)$ can be calculated from $\tilde{\phi}$ as follows:

$$\tilde{C}_p(\hat{x},\hat{z},\hat{t}) = - \frac{2}{U_\infty^2} \cdot \left(\frac{\partial}{\partial \hat{t}} + U_\infty \cdot \frac{\partial}{\partial \hat{x}}\right) \tilde{\hat{\phi}}(\hat{x},\hat{z},\hat{t}) \, . \tag{21}$$

Substituting Equation (8) for $\tilde{\hat{\phi}}$ in the above equation gives

$$\tilde{C}_p(\hat{x},\hat{z}) = \tilde{C}_{p0}(\hat{x},\hat{z}) + \tilde{C}_{pc}(\hat{x},\hat{z}) \cdot \cos(\hat{\omega}\hat{t}) + \tilde{C}_{ps}(\hat{x},\hat{z}) \cdot \sin(\hat{\omega}\hat{t}) \, , \tag{22}$$

where

$$\tilde{C}_{p0}(\hat{x},\hat{z}) = - \frac{2}{U_\infty} \cdot \frac{\partial \tilde{\hat{\phi}}_0}{\partial \hat{x}} \, , \tag{23}$$

$$\tilde{C}_{pc}(\hat{x},\hat{z}) = - \frac{2}{U_\infty} \cdot \left(\frac{\partial \tilde{\hat{\phi}}_c}{\partial \hat{x}} + \frac{\hat{\omega}}{U_\infty} \cdot \tilde{\hat{\phi}}_s\right) , \tag{24}$$

and

$$\tilde{C}_{ps}(\hat{x},\hat{z}) = - \frac{2}{U_\infty} \cdot \left(\frac{\partial \tilde{\hat{\phi}}_s}{\partial \hat{x}} - \frac{\hat{\omega}}{U_\infty} \cdot \tilde{\hat{\phi}}_c\right) . \tag{25}$$

With the aid of Equation (14), Equations (24) and (25) can be combined into one expression:

$$\tilde{C}_p(\hat{x},\hat{z}) = -\frac{2}{\beta}\cdot\left(\frac{1}{\beta}\cdot\frac{\partial}{\partial x} - \frac{\omega}{M_\infty}\,i\right)\tilde{\phi}^* \,, \tag{26}$$

where

$$\tilde{C}_p = \tilde{C}_{pc} + i\,\tilde{C}_{ps} \,. \tag{27}$$

Solving Equation (26) for $\tilde{\phi}^*$ with the boundary condition:

$$\tilde{\phi}^*(x,z) = 0 \text{ infinite upstream,} \tag{28}$$

gives

$$\tilde{\phi}^*(x,z) = -\frac{\beta^2}{2}\int_{-\infty}^{x}\tilde{C}_p(c\xi,\frac{c}{\beta}z)\cdot e^{-i\left(\frac{\omega\beta}{M_\infty}\xi - \frac{\omega}{M_\infty\beta}x\right)}\,d\xi \,. \tag{29}$$

From Equation (20) follows

$$[\tilde{\phi}^*]^+_- = -\frac{\beta^2}{2}\int_{-\infty}^{x}\tilde{CP}(c\xi)\cdot e^{-i\left(\frac{\omega\beta}{M_\infty}\xi - \frac{\omega}{M_\infty\beta}\cdot x\right)}\,d\xi \,, \tag{30}$$

where

$$\tilde{CP}(\hat{x}) = \Delta\tilde{C}_{pc}(\hat{x}) + i\,\Delta\tilde{C}_{ps}(\hat{x}) \,. \tag{31}$$

$\Delta\tilde{C}_{pc}$ and $\Delta\tilde{C}_{ps}$ are defined as

$$\Delta\tilde{C}_p(\hat{x},\hat{t}) = \Delta\tilde{C}_{p0}(\hat{x}) + \Delta\tilde{C}_{pc}(\hat{x})\cdot\cos(\hat{\omega}\hat{t}) + \Delta\tilde{C}_{ps}(\hat{x})\cdot\sin(\hat{\omega}\hat{t}), \tag{32}$$

where $\Delta\tilde{C}_p(\hat{x},\hat{t})$ is the time-dependent pressure coefficient difference at $\hat{x}$ between the upper and lower surfaces of the airfoil.

Differentiating both sides of Equation (19) with respect to z and substituting Equation (30) for $[\tilde{\phi}^*]^+_-$ in Equation (19) after letting z tend to zero give the following expression

$$\frac{1}{U_\infty}\cdot\tilde{w}(\hat{x}) = v.p.\int_{x_L}^{x_T}\tilde{CP}(c\xi)\cdot\tilde{K}(\xi-x)\,d\xi \,, \tag{33}$$

where

$$\tilde{K}(x) = \tilde{K}_r(x) + i\,\tilde{K}_i(x) \,. \tag{34}$$

and $\hat{k}$ is the reduced frequency defined as

$$\hat{k} = \frac{c\hat{\omega}}{2U_\infty} \,. \tag{35}$$

$\tilde{K}_r$ and $\tilde{K}_i$ are also defined as

$$\begin{aligned}\tilde{K}_r(x) = {} & \frac{\hat{k}}{4}\cdot\cos(2\hat{k}x) - \frac{\beta}{4\pi}\cdot\frac{1}{x}\cdot\cos\left(2\frac{\hat{k}}{\beta^2}x\right)\cdot\cos\left\{2\frac{\hat{k}}{\beta^2}(M_\infty-\beta^2)x\right\} \\ & - \frac{\hat{k}M_\infty}{4\pi\beta}\int_1^\infty\left(\frac{\sqrt{\theta^2-1}}{\theta+\frac{1}{M_\infty}}-1\right)\cdot\sin\left\{2\frac{\hat{k}M_\infty}{\beta^2}(\theta+M_\infty)x\right\}d\theta \\ & - \frac{\hat{k}M_\infty}{4\pi\beta}\int_{\frac{2}{M_\infty}-1}^\infty\left(\frac{\sqrt{\theta^2-1}}{\theta-\frac{1}{M_\infty}}-1\right)\cdot\sin\left\{2\frac{\hat{k}M_\infty}{\beta^2}(\theta-M_\infty)x\right\}d\theta \\ & - \frac{\hat{k}M_\infty}{4\pi\beta}\cdot\cos(2\hat{k}x)\int_{\frac{1}{M_\infty}}^{\frac{2}{M_\infty}-1}\frac{\sqrt{\theta^2-1}+\sqrt{\left(\frac{2}{M_\infty}-\theta\right)^2-1}}{\theta-\frac{1}{M_\infty}}\cdot\sin\left\{2\frac{\hat{k}M_\infty}{\beta^2}(\theta-\frac{1}{M_\infty})x\right\}d\theta \\ & - \frac{\hat{k}}{\pi\beta}\cdot\sin(2\hat{k}x)\int_{\frac{1}{M_\infty}}^{\frac{2}{M_\infty}-1}\frac{\cos\left\{2\frac{\hat{k}M_\infty}{\beta^2}(\theta-\frac{1}{M_\infty})x\right\}}{\sqrt{\theta^2-1}+\sqrt{\left(\frac{2}{M_\infty}-\theta\right)^2-1}}d\theta,\end{aligned} \tag{36}$$

$$\begin{aligned}\tilde{K}_i(x) = {} & -\frac{\hat{k}}{4}\cdot\sin(2\hat{k}x) - \frac{\beta}{4\pi}\cdot\frac{1}{x}\cdot\cos\left(2\frac{\hat{k}}{\beta^2}x\right)\cdot\sin\left\{2\frac{\hat{k}}{\beta^2}(M_\infty-\beta^2)x\right\} \\ & + \frac{\hat{k}M_\infty}{4\pi\beta}\int_1^\infty\left(\frac{\sqrt{\theta^2-1}}{\theta+\frac{1}{M_\infty}}-1\right)\cdot\cos\left\{2\frac{\hat{k}M_\infty}{\beta^2}(\theta+M_\infty)x\right\}d\theta \\ & - \frac{\hat{k}M_\infty}{4\pi\beta}\int_{\frac{2}{M_\infty}-1}^\infty\left(\frac{\sqrt{\theta^2-1}}{\theta-\frac{1}{M_\infty}}-1\right)\cdot\cos\left\{2\frac{\hat{k}M_\infty}{\beta^2}(\theta-M_\infty)x\right\}d\theta \\ & + \frac{\hat{k}M_\infty}{4\pi\beta}\cdot\sin(2\hat{k}x)\int_{\frac{1}{M_\infty}}^{\frac{2}{M_\infty}-1}\frac{\sqrt{\theta^2-1}+\sqrt{\left(\frac{2}{M_\infty}-\theta\right)^2-1}}{\theta-\frac{1}{M_\infty}}\cdot\sin\left\{2\frac{\hat{k}M_\infty}{\beta^2}(\theta-\frac{1}{M_\infty})x\right\}d\theta \\ & - \frac{\hat{k}}{\pi\beta}\cdot\cos(2\hat{k}x)\int_{\frac{1}{M_\infty}}^{\frac{2}{M_\infty}-1}\frac{\cos\left\{2\frac{\hat{k}M_\infty}{\beta^2}(\theta-\frac{1}{M_\infty})x\right\}}{\sqrt{\theta^2-1}+\sqrt{\left(\frac{2}{M_\infty}-\theta\right)^2-1}}d\theta.\end{aligned} \tag{37}$$

$\tilde{w}(\hat{x})$ has been defined as

$$\tilde{w}(\hat{x}) = \tilde{w}_c(\hat{x}) + i\,\tilde{w}_s(\hat{x}), \tag{38}$$

where the upwash $\tilde{w}(\hat{x},\hat{t})$ along the airfoil is expressed as follows:

$$\tilde{w}(\hat{x},\hat{t}) = \tilde{w}_c(\hat{x})\cdot\cos(\hat{\omega}\hat{t}) + \tilde{w}_s(\hat{x})\cdot\sin(\hat{\omega}\hat{t}). \tag{39}$$

Because the airfoil is in pitching motion expressed in Equation (1), $\tilde{w}_c$ and $\tilde{w}_s$ can be calculated easily and given as

$$\tilde{w}(\hat{x}) = -\tilde{\alpha}_A\left\{2\hat{k}\cdot\frac{\hat{x}}{c}\cdot\cos(\hat{\omega}\Delta\hat{\tau})-\sin(\hat{\omega}\Delta\hat{\tau})\right\} - i\,\tilde{\alpha}_A\left\{\cos(\hat{\omega}\Delta\hat{\tau})+2\hat{k}\cdot\frac{\hat{x}}{c}\cdot\sin(\hat{\omega}\Delta\hat{\tau})\right\}. \tag{40}$$

From Equation (33) the pressure distribution on the same airfoil model in a different pitching motion in a wind tunnel can be obtained. The uniform flow condition infinite upstream in the tunnel is the same as in the free air and the angular velocity of the motion and the fixed point are the same and the same xz co-ordinate system can be used. However, the time origin is not defined in the same way as in the free air. In this case, the time when the position of the airfoil coincides with its time-averaged position is defined as $\hat{t} = 0$. The angle of attack α for the airfoil in the tunnel can be written as follows:

$$\alpha(\hat{t}) = \alpha_0 + \alpha_A \cdot \sin(\hat{\omega}\hat{t}) \ . \tag{41}$$

The half height of the tunnel is $\hat{H}$ and the fixed point for the pitching motion is on the tunnel center line in this paper (see Fig. 2). The small disturbance potential function $\hat{\phi}$ for the flow field in the tunnel disturbed by the airfoil also satisfies Equation (2) like $\tilde{\hat{\phi}}$. Here $\hat{\phi}$ is defined from the full velocity potential function $\hat{\Phi}$ as follows:

$$\hat{\Phi} = U_\infty \cdot \hat{x} + \hat{\phi} \ , \tag{42}$$

Introduce a new function ϕ related to $\hat{\phi}$ by the following:

$$\beta^2 \hat{\phi} = c \cdot U_\infty \cdot \phi \ . \tag{43}$$

This results in the following:

$$\nabla^2 \phi^* + \kappa^2 \cdot \phi^* = 0 \ , \tag{44}$$

where

$$\phi^* = (\phi_c + i\phi_s) \cdot e^{i \frac{\omega M_\infty}{\beta} \cdot x} \ . \tag{45}$$

ϕ_c and ϕ_s are the time-dependent cosine and sine terms similar to $\tilde{\phi}_c$ and $\tilde{\phi}_s$ in Equation (10). Using Green's theorem, the following expression for ϕ^* can be obtained:

$$\iint_\Omega (\phi^* \cdot \nabla^2 \psi - \psi \cdot \nabla^2 \phi^*) \, d\Omega = \oint_{\partial\Omega} \left(\phi^* \cdot \frac{\partial \psi}{\partial n} - \psi \cdot \frac{\partial \phi^*}{\partial n}\right) ds \ , \tag{46}$$

where ψ is an analytical real-valued function and the other conditions have been described in Equation (16). Let ψ be written as

$$\begin{aligned} \psi(\xi,\zeta;x,z) = \tilde{\psi}(\xi,\zeta;x,z) \\ + \frac{1}{2\pi} \lim_{\varepsilon \to 0+} \Big[v.p. \int_0^{1-\varepsilon} \frac{1}{\sqrt{1-\theta^2}} \cdot \cot\{\kappa H \sqrt{1-\theta^2}\} \cdot \cos\{\kappa|\zeta - z|\sqrt{1-\theta^2}\} \cdot \cos\{\kappa(\xi - x)\theta\} \, d\theta \\ - \int_{1+\varepsilon}^{\infty} \frac{1}{\sqrt{\theta^2-1}} \cdot \coth(\kappa H \sqrt{\theta^2-1}) \cdot \frac{e^{-\kappa H\sqrt{\theta^2-1}}}{\cosh(\kappa H \sqrt{\theta^2-1})} \cdot \cosh\{\kappa|\zeta - z|\sqrt{\theta^2-1}\} \cdot \cos\{\kappa(\xi - x)\theta\} \, d\theta \Big] \ , \end{aligned} \tag{47}$$

then this function is continuous and differentiable two times with ξ and ζ except at the point (x,z) within the following band:

$$|\zeta - z| < 2H \ . \tag{48}$$

Also,

$$\kappa H \neq n\pi \ ; \ n = 0, \pm 1, \pm 2, \ldots \tag{49}$$

since the principal value of the integral must exist. ψ is satisfied by the equation

$$\nabla^2 \psi + \kappa^2 \cdot \psi = 0 \ , \tag{50}$$

Hence, Equation (46) becomes

$$\phi^*(x,z) = -\int_{x_L}^{\infty} [\phi^*]_-^+ \cdot \frac{\partial \psi}{\partial \zeta}\Big|_{\zeta=0} d\xi + \int_{-\infty}^{\infty} [\phi^*]_{-H}^{H} \cdot \frac{\partial \psi}{\partial \zeta}\Big|_{\zeta=-H} d\xi - \int_{-\infty}^{\infty} [\frac{\partial \phi^*}{\partial \zeta}]_{-H}^{H} \cdot \psi|_{\zeta=-H} d\xi \,. \quad (51)$$

Appendix B can be referred to for the detail derivation. In the same way as $\tilde{\phi}^*$,

$$[\phi^*]_-^+ = -\frac{\beta^2}{2}\int_{-\infty}^{x} \mathbf{CP}(c\xi)\cdot e^{-i\left(\frac{\omega\beta}{M_\infty}\xi - \frac{\omega}{M_\infty\beta}x\right)} d\xi \,, \quad (52)$$

where

$$\mathbf{CP}(\hat{x}) = \Delta C_{pc}(\hat{x}) + i\,\Delta C_{ps}(\hat{x}) \,. \quad (53)$$

ΔC_{pc} and ΔC_{ps} are the time-dependent cosine and sine components of the pressure difference between the upper and lower airfoil surface similar to $\Delta\tilde{C}_{pc}$ and $\Delta\tilde{C}_{ps}$. As in the expression for $[\phi^*]_-^+$,

$$[\phi^*]_{-H}^{H} = -\frac{\beta^2}{2}\int_{-\infty}^{x} \mathbf{CH}(c\xi)\cdot e^{-i\left(\frac{\omega\beta}{M_\infty}\xi - \frac{\omega}{M_\infty\beta}x\right)} d\xi \,, \quad (54)$$

where

$$\mathbf{CH}(\hat{x}) = [C_{pc}(\hat{x},\hat{z})]_{-H}^{H} + i\,[C_{ps}(\hat{x},\hat{z})]_{-H}^{H} \,. \quad (55)$$

C_{pc}, C_{ps}, ΔC_{pc} and ΔC_{ps} are the time-dependent cosine and sine components. Noting the pressure difference between the upper and lower wind tunnel walls with $C_{pH}(\hat{x},\hat{t})$ and using a Fourier series expansion $\hat{t}$ gives

$$C_{pH}(\hat{x},\hat{t}) = C_{p0}^{H}(\hat{x}) + C_{pc}^{H}(\hat{x})\cdot\cos(\hat{\omega}\hat{t}) + C_{ps}^{H}(\hat{x})\cdot\sin(\hat{\omega}\hat{t}) \quad (56)$$

and hence,

$$\mathbf{CH}(\hat{x}) = C_{pc}^{H}(\hat{x}) + i\,C_{ps}^{H}(\hat{x}) \,. \quad (57)$$

Differentiating the both side of Equation (51) with z and substituting Equations (52) and (55) for $[\phi^*]_-^+$ and $[\phi^*]_{-H}^{H}$ into Equation (51) and letting z tend to zero give

$$\frac{w(\hat{x})}{U_\infty} = \text{v.p.}\int_{x_L}^{x_T} \mathbf{CP}(c\xi)\cdot K(\xi-x)\,d\xi - \int_{-\infty}^{\infty} \mathbf{CH}(c\xi)\cdot \mathbf{WA}(\xi-x)\,d\xi \,, \quad (58)$$

where

$$K(x) = (K_r + i K_i) + (\Delta K_r + i\Delta K_i) \,, \quad (59)$$

and

$$\mathbf{WA}(x) = W_r(x) + i\,W_i(x) \,. \quad (60)$$

From Equation (47) it follows

$$\Delta K_r(x) = \frac{\hat{k}}{4}\cdot\{\coth(2\hat{k}\hat{H})-1\}\cdot\cos(2\hat{k}x)$$
$$-\frac{\hat{k}M_\infty}{4\pi\beta}\,V.P.\int_0^1\frac{\sqrt{1-\theta^2}}{\theta+\frac{1}{M_\infty}}\cdot\cot\left(2\frac{\hat{k}M_\infty}{\beta}\hat{H}\sqrt{1-\theta^2}\right)\cdot\sin\left\{2\frac{\hat{k}M_\infty}{\beta^2}\cdot x(\theta+M_\infty)\right\}d\theta$$
$$-\frac{\hat{k}M_\infty}{4\pi\beta}\,V.P.\int_0^1\frac{\sqrt{1-\theta^2}}{\theta-\frac{1}{M_\infty}}\cdot\cot\left(2\frac{\hat{k}M_\infty}{\beta}\hat{H}\sqrt{1-\theta^2}\right)\cdot\sin\left\{2\frac{\hat{k}M_\infty}{\beta^2}x(\theta-M_\infty)\right\}d\theta$$
$$-\frac{\hat{k}M_\infty}{4\pi\beta}\int_1^\infty\frac{\sqrt{\theta^2-1}}{\theta+\frac{1}{M_\infty}}\cdot\left\{\coth\left(2\frac{\hat{k}M_\infty}{\beta}\hat{H}\sqrt{\theta^2-1}\right)-1\right\}\cdot\sin\left\{2\frac{\hat{k}M_\infty}{\beta^2}x(\theta+M_\infty)\right\}d\theta$$
$$-\frac{\hat{k}M_\infty}{4\pi\beta}\,V.P.\int_1^\infty\frac{\sqrt{\theta^2-1}}{\theta-\frac{1}{M_\infty}}\cdot\left\{\coth\left(2\frac{\hat{k}M_\infty}{\beta}\hat{H}\sqrt{\theta^2-1}\right)-1\right\}\cdot\sin\left\{2\frac{\hat{k}M_\infty}{\beta^2}x(\theta-M_\infty)\right\}d\theta, \qquad (61)$$

$$\Delta K_i(x) = -\frac{\hat{k}}{4}\cdot\{\coth(2\hat{k}\hat{H})-1\}\cdot\sin(2\hat{k}x)$$
$$+\frac{\hat{k}M_\infty}{4\pi\beta}\cdot V.P.\int_0^1\frac{\sqrt{1-\theta^2}}{\theta+\frac{1}{M_\infty}}\cdot\cot\left(2\frac{\hat{k}M_\infty}{\beta}\hat{H}\sqrt{1-\theta^2}\right)\cdot\cos\left\{2\frac{\hat{k}M_\infty}{\beta^2}\cdot x(\theta+M_\infty)\right\}d\theta$$
$$-\frac{\hat{k}M_\infty}{4\pi\beta}\,V.P.\int_0^1\frac{\sqrt{1-\theta^2}}{\theta-\frac{1}{M_\infty}}\cdot\cot\left(2\frac{\hat{k}M_\infty}{\beta}\hat{H}\sqrt{1-\theta^2}\right)\cdot\cos\left\{2\frac{\hat{k}M_\infty}{\beta^2}\cdot x(\theta-M_\infty)\right\}d\theta$$
$$+\frac{\hat{k}M_\infty}{4\pi\beta}\int_1^\infty\frac{\sqrt{\theta^2-1}}{\theta+\frac{1}{M_\infty}}\cdot\left\{\coth\left(2\frac{\hat{k}M_\infty}{\beta}\hat{H}\sqrt{\theta^2-1}\right)-1\right\}\cdot\cos\left\{2\frac{\hat{k}M_\infty}{\beta^2}\cdot x(\theta+M_\infty)\right\}d\theta$$
$$-\frac{\hat{k}M_\infty}{4\pi\beta}\,V.P.\int_1^\infty\frac{\sqrt{\theta^2-1}}{\theta-\frac{1}{M_\infty}}\cdot\left\{\coth\left(2\frac{\hat{k}M_\infty}{\beta}\cdot\hat{H}\sqrt{\theta^2-1}\right)-1\right\}\cdot\cos\left\{2\frac{\hat{k}M_\infty}{\beta^2}\cdot x(\theta-M_\infty)\right\}d\theta, \qquad (62)$$

$$W_r(x) = \frac{\hat{k}}{4}\cdot e^{-2\hat{k}\hat{H}}\cdot\{\coth(2\hat{k}\hat{H})+1\}\cdot\cos(2\hat{k}x)$$
$$-\frac{\hat{k}M_\infty}{4\pi\beta}\,V.P.\int_0^1\frac{\sqrt{1-\theta^2}}{\theta+\frac{1}{M_\infty}}\cdot\operatorname{cosec}\left(2\frac{\hat{k}M_\infty}{\beta}\hat{H}\sqrt{1-\theta^2}\right)\cdot\sin\left\{2\frac{\hat{k}M_\infty}{\beta^2}\cdot x(\theta+M_\infty)\right\}d\theta$$
$$-\frac{\hat{k}M_\infty}{4\pi\beta}\,V.P.\int_0^1\frac{\sqrt{1-\theta^2}}{\theta-\frac{1}{M_\infty}}\cdot\operatorname{cosec}\left(2\frac{\hat{k}M_\infty}{\beta}\hat{H}\sqrt{1-\theta^2}\right)\cdot\sin\left\{2\frac{\hat{k}M_\infty}{\beta^2}\cdot x(\theta-M_\infty)\right\}d\theta$$
$$-\frac{\hat{k}M_\infty}{4\pi\beta}\int_1^\infty\frac{\sqrt{\theta^2-1}}{\theta+\frac{1}{M_\infty}}\cdot e^{-2\frac{\hat{k}M_\infty}{\beta}\hat{H}\sqrt{\theta^2-1}}\cdot\left\{\coth\left(2\frac{\hat{k}M_\infty}{\beta}\hat{H}\sqrt{\theta^2-1}\right)+1\right\}\cdot\sin\left\{2\frac{\hat{k}M_\infty}{\beta^2}x(\theta+M_\infty)\right\}d\theta$$
$$-\frac{\hat{k}M_\infty}{4\pi\beta}\,V.P.\int_1^\infty\frac{\sqrt{\theta^2-1}}{\theta-\frac{1}{M_\infty}}\cdot e^{-2\frac{\hat{k}M_\infty}{\beta}\hat{H}\sqrt{\theta^2-1}}\cdot\left\{\coth\left(2\frac{\hat{k}M_\infty}{\beta}\hat{H}\sqrt{\theta^2-1}\right)+1\right\}\cdot\sin\left\{2\frac{\hat{k}M_\infty}{\beta^2}x(\theta-M_\infty)\right\}d\theta, \qquad (63)$$

and

$$
\begin{aligned}
W_i(x) \;=\; & -\frac{\hat{k}}{4}\cdot e^{-2\hat{k}\hat{H}}\cdot\{\coth(2\hat{k}\hat{H})+1\}\cdot\sin(2\hat{k}x) \\
& + \frac{\hat{k}M_\infty}{4\pi\beta}\,v.p.\int_0^1 \frac{\sqrt{1-\theta^2}}{\theta+\frac{1}{M_\infty}}\cdot\operatorname{cosec}\left(2\,\frac{\hat{k}M_\infty}{\beta}\hat{H}\sqrt{1-\theta^2}\right)\cdot\cos\left\{2\,\frac{\hat{k}M_\infty}{\beta^2}\cdot x(\theta+M_\infty)\right\}d\theta \\
& - \frac{\hat{k}M_\infty}{4\pi\beta}\,v.p.\int_0^1 \frac{\sqrt{1-\theta^2}}{\theta-\frac{1}{M_\infty}}\cdot\operatorname{cosec}\left(2\,\frac{\hat{k}M_\infty}{\beta}\hat{H}\sqrt{1-\theta^2}\right)\cdot\cos\left\{2\,\frac{\hat{k}M_\infty}{\beta^2}\,x(\theta-M_\infty)\right\}d\theta \\
& + \frac{\hat{k}M_\infty}{4\pi\beta}\int_1^\infty \frac{\sqrt{\theta^2-1}}{\theta+\frac{1}{M_\infty}}\cdot e^{-2\frac{\hat{k}M_\infty}{\beta}\hat{H}\sqrt{\theta^2-1}}\cdot\left\{\coth\left(2\,\frac{\hat{k}M_\infty}{\beta}\hat{H}\sqrt{\theta^2-1}\right)+1\right\}\cos\left\{2\,\frac{\hat{k}M_\infty}{\beta^2}x(\theta+M_\infty)\right\}d\theta \\
& - \frac{\hat{k}M_\infty}{4\pi\beta}\,v.p.\int_1^\infty \frac{\sqrt{\theta^2-1}}{\theta-\frac{1}{M_\infty}}\cdot e^{-2\frac{\hat{k}M_\infty}{\beta}\hat{H}\sqrt{\theta^2-1}}\cdot\left\{\coth\left(2\,\frac{\hat{k}M_\infty}{\beta}\hat{H}\sqrt{\theta^2-1}\right)+1\right\}\cdot\cos\left\{2\,\frac{\hat{k}M_\infty}{\beta^2}x(\theta-M_\infty)\right\}d\theta . \qquad (64)
\end{aligned}
$$

Some examples of ΔK and WA are shown in Figures 3 to 8. $w(\hat{x})$ has been defined as

$$
w(\hat{x}) \;=\; w_c(\hat{x}) + i\,w_s(\hat{x}) , \qquad (65)
$$

where the upwash $w(\hat{x},\hat{t})$ along the airfoil is expressed as follows:

$$
w(\hat{x},\hat{t}) = w_0(\hat{x}) + w_c(\hat{x})\cdot\cos(\hat{\omega}\hat{t}) + w_s(\hat{x})\cdot\sin(\hat{\omega}\hat{t}) . \qquad (66)
$$

From Equation (41) it follows that

$$
w(\hat{x}) \;=\; -2\alpha_A\cdot\hat{k}\cdot\frac{\hat{x}}{c} - i\,\alpha_A \;. \qquad (67)
$$

Subtracting Equation (33) from Equation (67) gives

$$
\begin{aligned}
\frac{1}{U_\infty}\Delta w(\hat{x}) \;=\; & \int_{x_L}^{x_T} CP(c\xi)\cdot\Delta K(\xi-x)\,d\xi - \int_{-\infty}^{\infty} CH(c\xi)\cdot WA(\xi-x)\,d\xi \\
& + v.p.\int_{x_L}^{x_T}\Delta CP(c\xi)\cdot\tilde{K}(\xi-x)\,d\xi \;, \qquad (68)
\end{aligned}
$$

where

$$
\Delta w(\hat{x}) \;=\; w(\hat{x}) - \tilde{w}(\hat{x}) , \qquad (69)
$$

$$
\Delta K(x) \;=\; \Delta K_r(x) + i\,\Delta K_i , \qquad (70)
$$

and

$$
\Delta CP(\hat{x}) \;=\; CP(\hat{x}) - \widetilde{CP}(\hat{x}) . \qquad (71)
$$

It should be noted here that CP ($\hat{x}$) and CH ($\hat{x}$) and w ($\hat{x}$) can be measured in a wind tunnel test but $\widetilde{CP}(\hat{x})$ and $\tilde{\alpha}_A$ and $\Delta\tau$ are unknown. The unknown quantities in Equation (68) are $\Delta CP(x)$, $\tilde{\alpha}_A$ with $\Delta\tau$ being an arbitrary parameter. The aim in the wind tunnel wall correction is to obtain interference-free data from the test data. Therefore, it is better for CP and $\widetilde{CP}$ to be close to each other because

there is the possibility that the difference between CP and $\widetilde{CP}$ can generate completely different flow field from each other due to the coupling between viscous and inviscid flow regions such as the separated flow. As a result, $\widetilde{\alpha}_A$ and $\Delta\tau$ must be chosen so that ΔCP may be as small as possible. ΔCP is a function of x and the magnitude of it depends on its definition. Equation (68) reduces to

$$v.p. \int_{x_L}^{x_T} \Delta CP(c\xi) \cdot \widetilde{K}(\xi - x)\, d\xi = \frac{w_i(\hat{x})}{U_\infty} + \frac{\Delta w(\hat{x})}{U_\infty} , \tag{72}$$

where

$$\frac{w_i(\hat{x})}{U_\infty} = -\int_{x_L}^{x_T} CP(c\xi) \cdot \Delta K(\xi - x)\, d\xi + \int_{-\infty}^{\infty} CH(c\xi) \cdot WA(\xi - x)\, d\xi . \tag{73}$$

In this paper, $\widetilde{\alpha}_A$ and $\Delta\tau$ are chosen so that the following function may be a minimum:

$$I(\widetilde{\alpha}_A, \Delta\tau) = \int_{x_L}^{x_T} | w_i + \Delta w |^2 \, d\xi . \tag{74}$$

It will be studied in the next section whether these values of $\widetilde{\alpha}_A$ and $\Delta\tau$ are satisfactory. Then

$$\frac{\partial I}{\partial \widetilde{\alpha}_A} = 0 , \tag{75}$$

and

$$\frac{\partial I}{\partial \Delta\tau} = 0 . \tag{76}$$

From Equations (40), (67) and (69) it follows

$$\tan(\hat{\omega}\Delta\tau) = \frac{\overline{f_c} - 2\hat{k}\,\overline{x f_s}}{\alpha_A(1 + 4\hat{k}^2 \cdot \overline{x^2}) - (\overline{f_s} + 2\hat{k} \cdot \overline{x f_c})} , \tag{77}$$

where

$$\frac{w_i}{U_\infty} = f_c + i\, f_s , \tag{78}$$

and $(\bar{\ })$ means the averaged value over the airfoil chord.

Also,

$$\widetilde{\alpha}_A - \alpha_A = \{\cos(\hat{\omega}\Delta\tau) - 1\} \cdot \alpha_A + \frac{1}{1 + 4\hat{k}^2 \cdot \overline{x^2}} \cdot \{(\overline{f_c} - 2\hat{k} \cdot \overline{x f_s}) \cdot \sin(\hat{\omega}\Delta\tau) - (\overline{f_s} + 2\hat{k} \cdot \overline{x f_c}) \cdot \cos(\hat{\omega}\Delta\tau)\} . \tag{79}$$

Because the values of $\Delta\tau$ and $\tilde{\alpha}_A$ can be calculated with the aid of Equations (77) and (79), the right-hand side of Equation (72) can be estimated. If the value of the term in Equation (72) is small enough over the airfoil to be neglected within the accuracy of the test condition, ΔCP can be also neglected. In this case, the tunnel test data can be corrected in the sense of wind tunnel wall interference. However, not all tunnel test data can be corrected. In such circumstances, it is necessary to solve the integral equation Equation (72) for $\Delta CP(x)$ and to get $\widetilde{CP}(x)$ with the aid of Equation (71). However such additional correction is not recommended because it is desirable that tunnel test data are affected as little as possible. In addition to the correction mensioned in this paper, the correction corresponding to the time-averaged flow must be made. This correction is the same as that for steady flow. The terms f_c and f_i on the right-hand side of Equation (78) can be calculated from Equation (73) with the aid of Equations (61) to (64).

The wall interference on an airfoil in plunging motion can be estimated in a similar way as that for pitching motion. The time and space co-ordinate system is the same as in the previous case. The z-co-ordinate of the mean camber of the airfoil model in the motion in free air, $\widetilde{S}_c(\hat{x},\hat{t})$, is

$$\widetilde{S}_c(\hat{x},\hat{t}) = S_{c_0}(\hat{x}) + \widetilde{h}_A \cdot \sin\{\hat{\omega}\cdot(\hat{t}-\Delta\hat{\tau})\}\ , \tag{80}$$

where S_{c_0} means the mean camber of the airfoil itself and h_A is the amplitude of the plunging motion. In this case the upward velocity at a point on the airfoil is

$$\widetilde{w}(\hat{x},\hat{t}) = \widetilde{h}_A\hat{\omega}\cdot\cos\{\hat{\omega}\cdot(\hat{t}-\Delta\hat{\tau})\}\ . \tag{81}$$

Using this definition for $\widetilde{w}(\hat{x})$, it follows

$$\widetilde{w}(\hat{x}) = \widetilde{h}_A\cdot\hat{\omega}\cdot\cos(\hat{\omega}\Delta\hat{\tau}) + i\,\widetilde{h}_A\cdot\hat{\omega}\cdot\sin(\hat{\omega}\Delta\hat{\tau})\ . \tag{82}$$

Consider the same airfoil model in the plunging motion installed in a wind tunnel. The angular velocity is also the same as $\hat{\omega}$, and the z-co-ordinate of the mean camber, $S_c(\hat{x},\hat{t})$, is

$$S_c(\hat{x},\hat{t}) = S_{c_0}(\hat{x}) + h_A\cdot\sin(\hat{\omega}\hat{t})\ . \tag{83}$$

From Equations (65) and (66),

$$w(\hat{x}) = h_A\cdot\hat{\omega}\ . \tag{84}$$

By the same method used in deriving corrections for pitching motion, the corrections for the plunging motion can be estimated. In this case, the estimation function I in Equation (74) becomes a function of $\widetilde{h}_A$ and $\Delta\tau$, that is,

$$I(\widetilde{h}_A,\Delta\hat{\tau}) = \int_{x_L}^{x_T} |w_i(c\xi)+\Delta w(c\xi)|^2\,d\xi\ . \tag{85}$$

This function must be minimum with respect to both $\widetilde{h}_A$ and $\Delta\tau$:

$$\frac{\partial I}{\partial \widetilde{h}_A} = 0\ , \tag{86}$$

and

$$\frac{\partial I}{\partial \Delta\hat{\tau}} = 0\ . \tag{87}$$

From Equations (85) to (87),

$$\tan(\hat{\omega}\Delta\hat{\tau}) = \frac{\bar{f}_s}{\bar{f}_c + 2\hat{k}\cdot h_A/c}, \tag{88}$$

and

$$\widetilde{h}_A - h_A = \{\cos(\hat{\omega}\Delta\hat{\tau}) - 1\}\cdot h_A + \frac{c}{2\hat{k}}\cdot\{\bar{f}_c\cdot\cos(\hat{\omega}\Delta\hat{\tau}) + \bar{f}_s\cdot\sin(\hat{\omega}\Delta\hat{\tau})\}. \tag{89}$$

3. SOME EXAMPLES OF CORRECTION

Some examples of wall corrections using the new method are described here. It should be noticed here that the examples indicate only the process of using the method and its limitations, but that they cannot prove the validity of the method. This method has been already proved analytically on the base of some of the assumptions mentioned in the previous section. Many experiments have indicated these assumptions are reasonable and they have been adopted in many other papers.

For simplicity in the calculations, the wall interference in an open tunnel is investigated. In order to confirm the procedure of solving Equation (33) to be correct, the pressure distributions on the oscillating airfoil in pitching motion are calculated using a numerical method. The airfoil is installed in an open tunnel having a half-height of 5.0. The uniform flow Mach number is 0.866. The airfoil chord length is 1.0 and the pitch axis is at the mid-chord point. The amplitude of the oscillating angle of attack is 1.0 degree. Ten values of the reduced frequency are adopted ranging from 0.02 to 0.18 in steps of 0.02 plus 0.17 because 0.182 is approximately the tunnel resonance frequency which can be calculated from Equation (49). The tunnel resonance frequency for the open tunnel cannot satisfy the condition given in Equation (49). The amplitude of C_L due to unit pitching motion with reduced frequency is shown in Figure 9, and the phase lag in C_L is shown in Figure 10. These quantities are calculated from the expression

$$|C_L|_\alpha = \frac{1}{\alpha}\cdot\sqrt{C_{Lc}^2 + C_{Ls}^2}, \tag{90}$$

and

$$\phi_{L\alpha} = \mathrm{Tan}^{-1}(C_{Ls}/C_{Lc}), \tag{91}$$

where

$$C_L(\hat{t}) = C_{L_0} + C_{Lc}\cdot\cos(\hat{\omega}\hat{t}) + C_{Ls}\cdot\sin(\hat{\omega}\hat{t}). \tag{92}$$

The two figures, Figures 9 and 10, show good agreement with the figures in Reference 3. This fact means the present solving process is right. Then suppose the data obtained by this numerical way to be data which should be corrected to data in the free air. In this case, the pressure coefficient on the tunnel walls is always zero. With the aid of Equations (77) and (79), the incidence amplitude and the phase lag in free air corresponding to the tunnel flow can be calculated from the pressure coefficient distribution on the airfoil in the open tunnel. Results are shown in Figures 11 and 12. The pressure coefficient difference between the upper and lower surfaces of the airfoil is

$$\Delta C_p(\hat{x},\hat{t}) = \Delta C_{p_0}(\hat{x}) + \Delta C_{pc}(\hat{x})\cdot\cos(\hat{\omega}\hat{t}) + \Delta C_{ps}(\hat{x})\cdot\sin(\hat{\omega}\hat{t}), \tag{93}$$

which has been defined at Equation (53). The time-dependent angle of attack is expressed:

$$\alpha(\hat{t}) = 0.0174533\cdot\sin(\hat{\omega}\hat{t}). \tag{94}$$

From Equation (1) follows

$$\tilde{\alpha}(\hat{t}) = \tilde{\alpha}_A \cdot \sin\{\hat{\omega}\cdot(\hat{t} - \Delta\tau)\} \cdot \tag{95}$$

For the pressure coefficient difference on the airfoil in the free air. This equation can be approximated by Equation (93) when the motion of the oscillating airfoil is defined by Equation (95), where $\tilde{\alpha}_A$ and $\hat{\omega}\Delta\tau$ can be calculated using Equations (77) and (79). If the airfoil in the free air oscillates in the same way as in the tunnel, that is,

$$\tilde{\alpha}(\tilde{\hat{t}}) = \tilde{\alpha}_A \cdot \sin(\hat{\omega}\,\tilde{\hat{t}}) \,, \tag{96}$$

the time variable $\hat{t}$ is transformed by

$$\hat{t} = \tilde{\hat{t}} + \Delta\tau \,. \tag{97}$$

The resultant expression for $\Delta\tilde{C}_p(\hat{x},\hat{t})$ can be written as:

$$\Delta\tilde{C}_p(\hat{x},\tilde{\hat{t}}) = \{\Delta C_{pc}(\hat{x})\cdot\cos(\hat{\omega}\Delta\tau) + \Delta C_{ps}(\hat{x})\cdot\sin(\hat{\omega}\Delta\tau)\}\cdot\cos(\hat{\omega}\,\tilde{\hat{t}})$$

$$+\{\Delta C_{ps}(\hat{x})\cdot\cos(\hat{\omega}\Delta\tau) - \Delta C_{pc}(\hat{x})\cdot\sin(\hat{\omega}\Delta\tau)\}\cdot\sin(\hat{\omega}\,\tilde{\hat{t}}) \tag{98}$$

In this way, the in-phase and out-of-phase components of the pressure coefficient difference as a function of the oscillating angle of attack can be calculated. By solving Equation (33) directly, $\Delta\tilde{C}_p$ can be obtained. Comparison between $\Delta\tilde{C}_p$ obtained from Equation (98) and Equation (33) provides a simple way for correcting $\tilde{\alpha}_A$ and $\Delta\tau$. The results are shown in Figures 13 to 14. These figures show that the method is suitable for low reduced frequencies but fails near the tunnel resonance frequencies. The time-dependent lift coefficient and pitching-moment coefficient about the pitch axis with the angle of attack are also shown in Figures 15 to 18. This example gives the extreme case because the uniform flow Mach number is 0.866. The next example is the same as in the previous case except for the Mach number and the tunnel height. The uniform flow Mach number is 0.600 and the tunnel semi-height is 4.0. In this case, the tunnel resonance reduced frequency is 0.52360. The reduced frequency was varied from 0.05 to 0.50 in steps of 0.05 and 0.52. Plots of $|\,C_L\,|_\alpha$ and $\phi_{L\alpha}$ with $\hat{k}$ are shown in Figures 19 and 20. The corrections, $(\tilde{\alpha}_A - \alpha_A)$ and $\omega\Delta\tau$, are shown in Figures 21 and 22 while Figures 23 to 24 show $\Delta\tilde{C}_p$ and Figures 25 to 28 show the C_L vs α and C_m vs α. These figures show also the same behaviour as in the previous case.

4. CONCLUSIONS

A new method of estimating the wind tunnel wall interference on an oscillating airfoil is presented. Instead of expressing the wall condition in unreliable ways, the time-dependent pressure distributions on the oscillating airfoil and near the tunnel walls in the flow direction are measured. With the aid of the measured pressure distributions, the corrections to the incidence amplitude and the phase lag, $(\hat{\omega}\Delta\tau)$, can be calculated by this new method. This method is very effective when the test is performed in a tunnel with ventilated walls because the unreliable expressions for the wall characteristics are not used at all in this method. The corrections are satisfactory except at reduced frequency near the tunnel resonance frequency. To determine whether corrections can be carried on by this method, it is necessary to check the induced upwash distribution on an airfoil due to the walls.

5. REFERENCES

1) Acum, W.E.A. — *Interference Effects in Unsteady Experiments.* ADARDograph 109, 1966.

2) Bland, S.R. — *The Two-Dimensional Oscillating Airfoil in a Wind in Subsonic Compressible Flow.* North Carolina State University at Raleigh, Ph.D., 1968 Mathematics.

3) Fromme, J.A. Goldberg, M.A. — *Unsteady Two-Dimensional Airloads Acting on Oscillating Thin Airfoils in Subsonic Ventilated Wind Tunnels.* NASA CR2967, 1978.

4) Fromme, J.A. Goldberg, M.A. — *Aerodynamic Interference Effects on Oscillating Airfoils with Controls in Ventilated Wind Tunnels.* AIAA Journal, Vol. 18, No. 4, April 1980, pp. 417, 426.

5) Fromme, J.A. Goldberg, M.A. — *Reformulation of Possio's Kernel with Application to Unsteady Wind Tunnel Interference.* AIAA Journal Vol. 18, No. 8, August 1980.

6) Kemp, W.B. — *Toward the Correctable Interference Transonic Wind Tunnel.* Proceedings of the AIAA 9th Aerodynamic Testing Conference, June 1976, pp. 31-38.

7) Capelier, C. Chevellier, J.-P. Bouniol, F. — *Nouvelle méthode de correction des effets de parios en courant pan.* La Recherche Aérospatiale, jan.-fév. 1978, pp. 1-11.

8) Lo, C.F. — *Tunnel Interference Assessment by Boundary Measurements.* AIAA Journal, Vol. 16, 1978, pp. 411-413.

9) Sawada, H. — *A General Correction Method of the Interference in Two-Dimensional Wind Tunnels with Ventilated Walls.* Transactions of the Japan Society for Aeronautical and Space Sciences, Vol. 21, 1978, pp. 57-68.

10) Mokry, M. Ohman, L.H. — *Application of the Fast Fourier Transform to Two-Dimensional Wind Tunnel Wall Interference.* Journal of Aircraft, Vol. 17, No. 6, 1980, pp. 402-408.

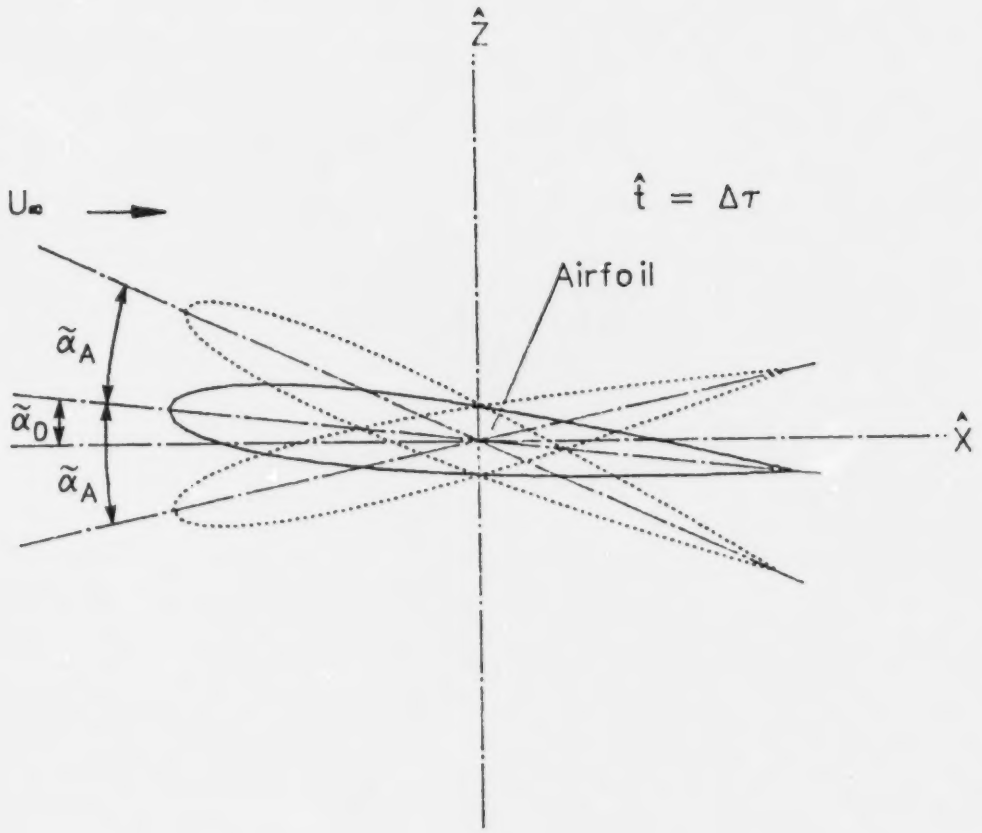

FIG. 1: AN AIRFOIL IN PITCHING MOTION IN FREE AIR

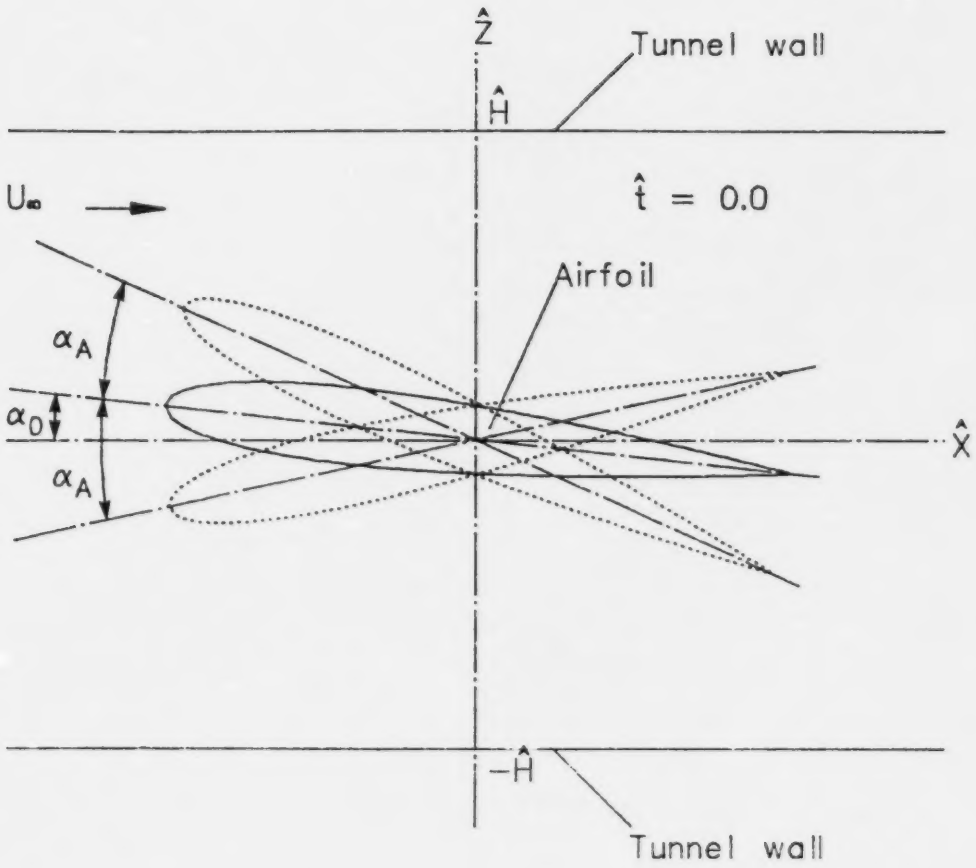

FIG. 2: AN AIRFOIL IN PITCHING MOTION IN A TUNNEL

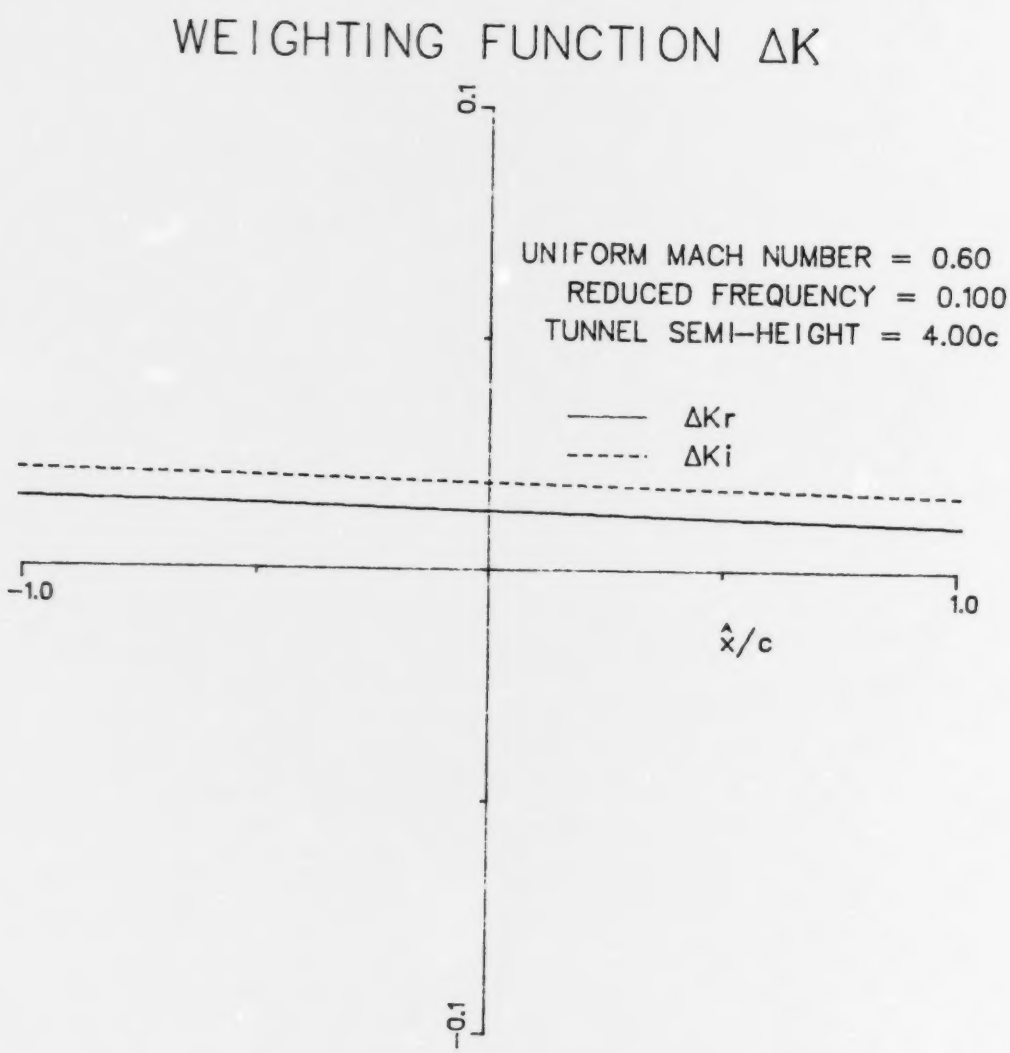

FIG. 3: ΔK vs $\hat{x}/c$

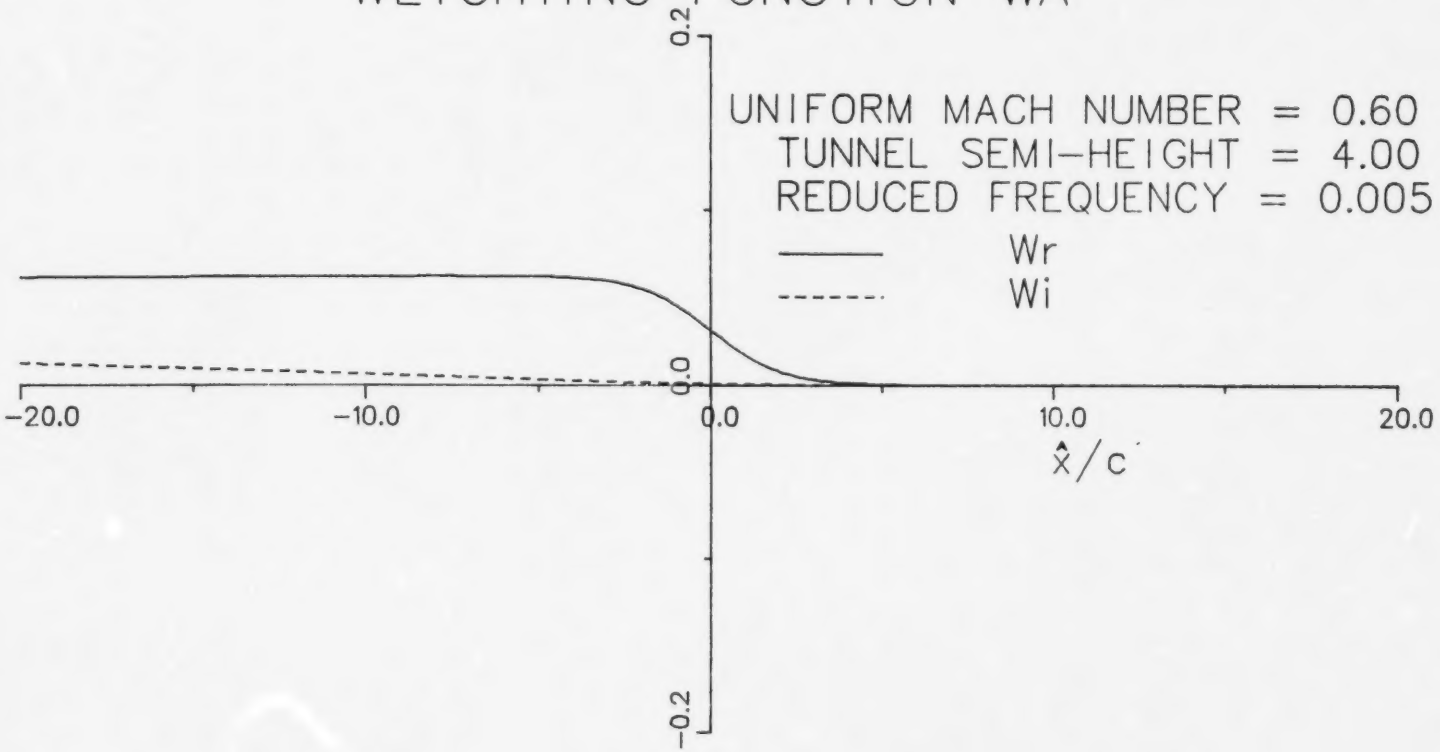

FIG. 4: WA vs $\hat{x}/c$

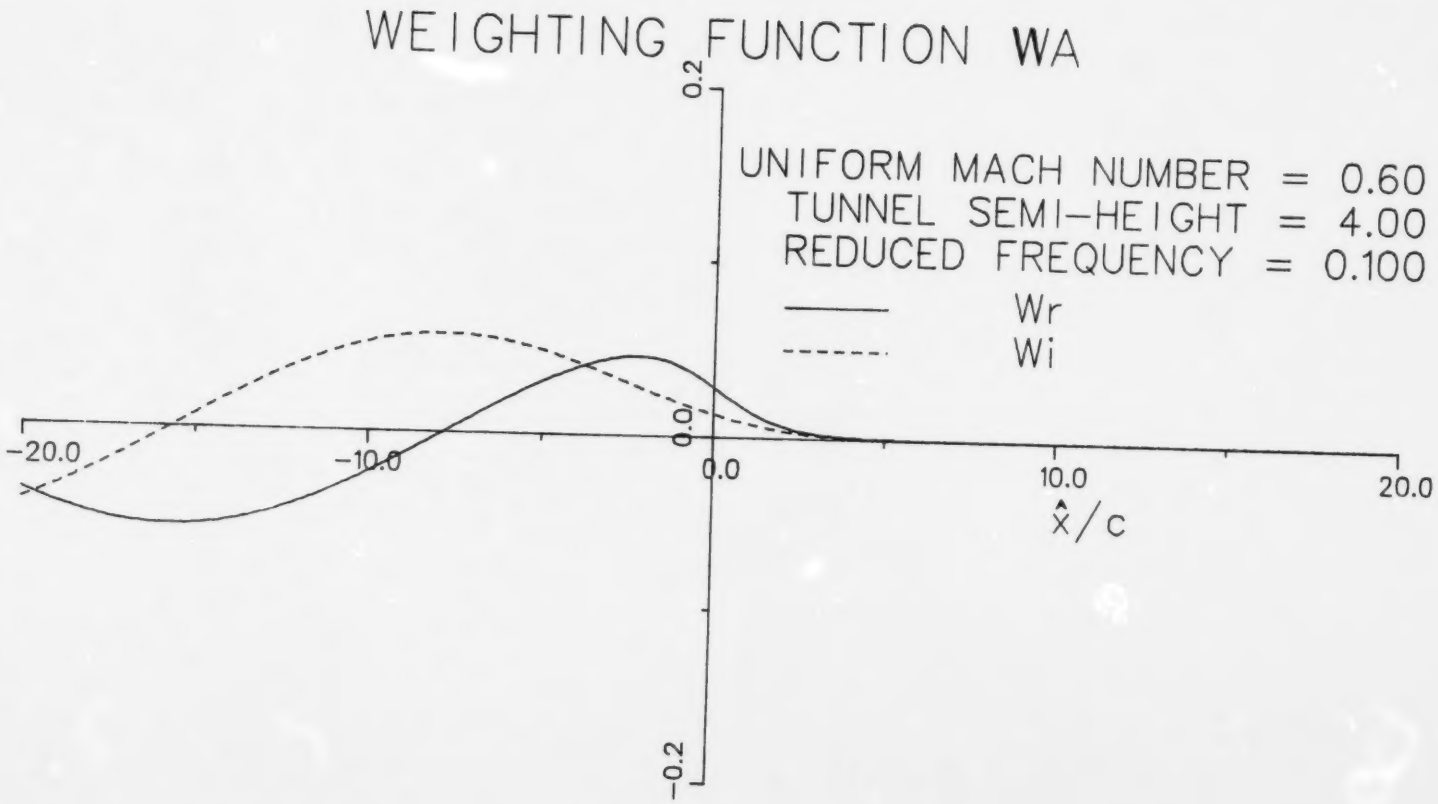

FIG. 5: WA vs $\hat{x}/c$

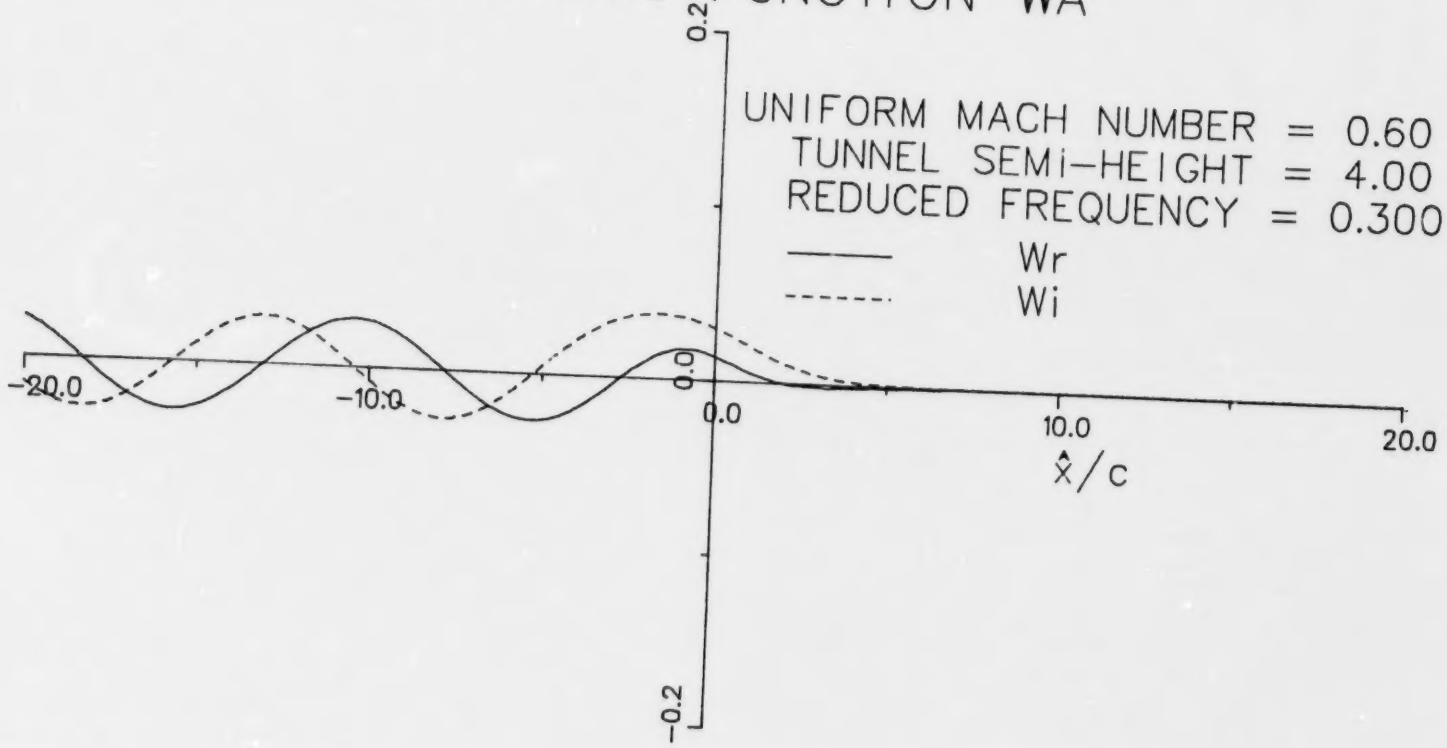

FIG. 6: WA vs $\hat{x}/c$

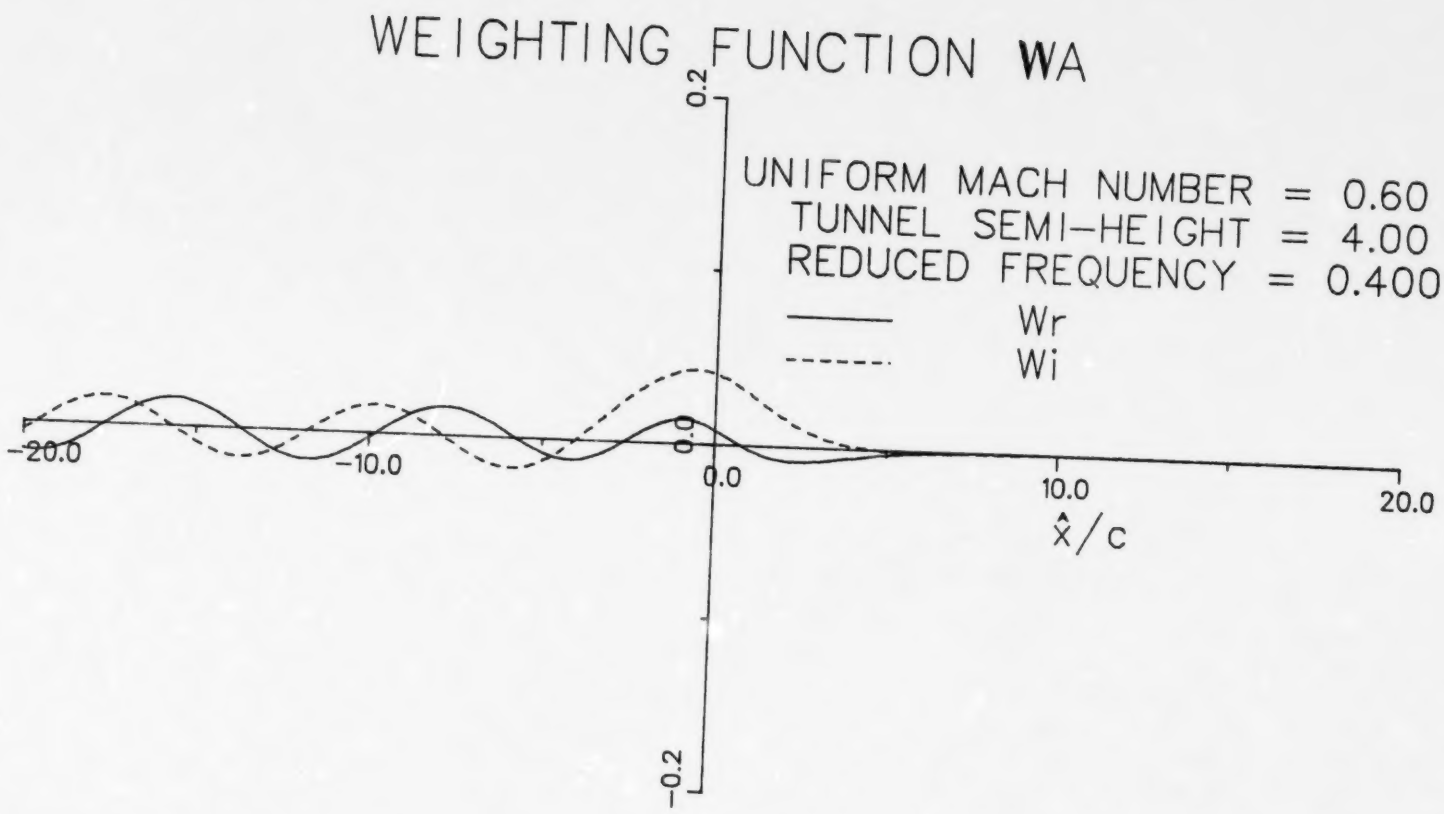

FIG. 7: WA vs $\hat{x}/c$

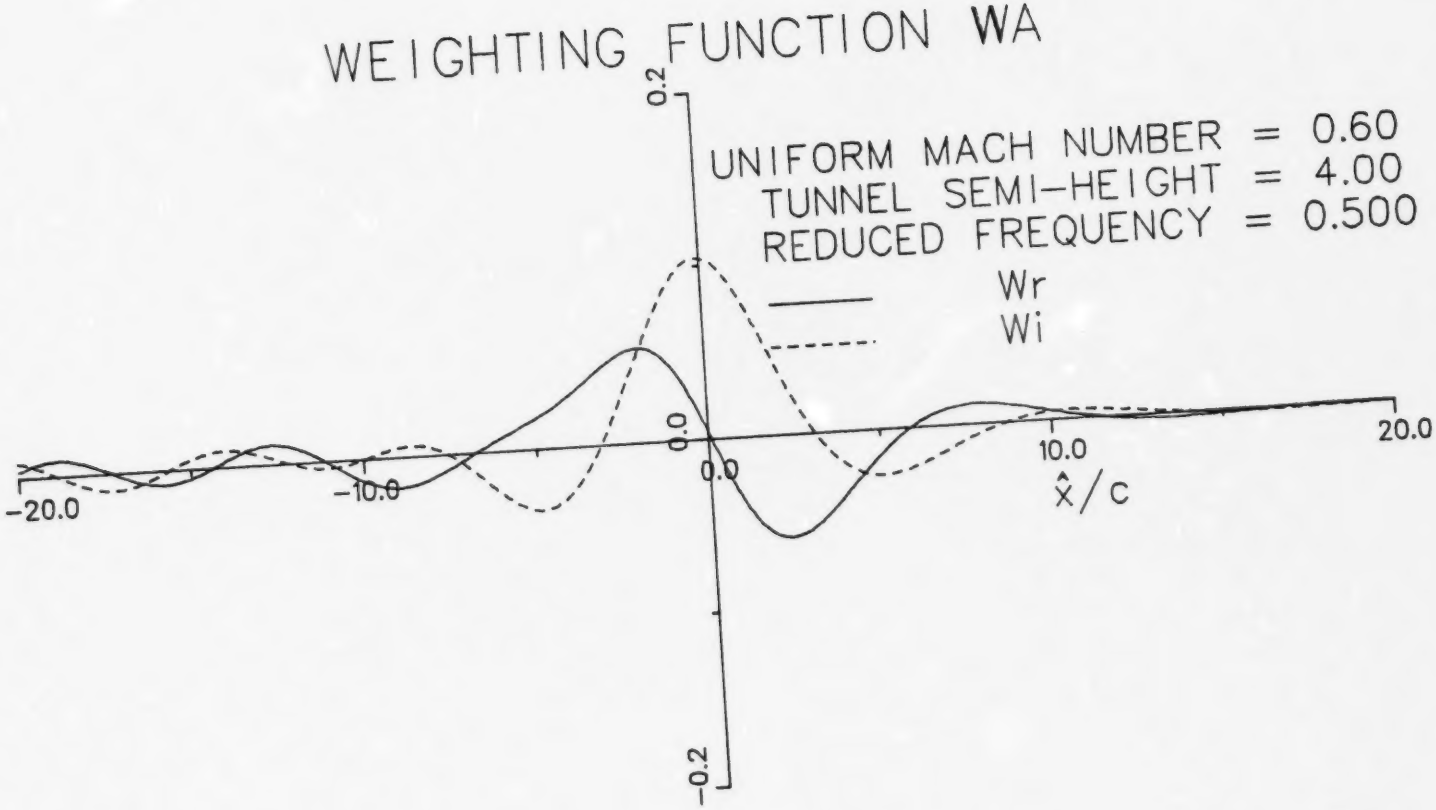

FIG. 8: WA vs $\hat{x}/c$

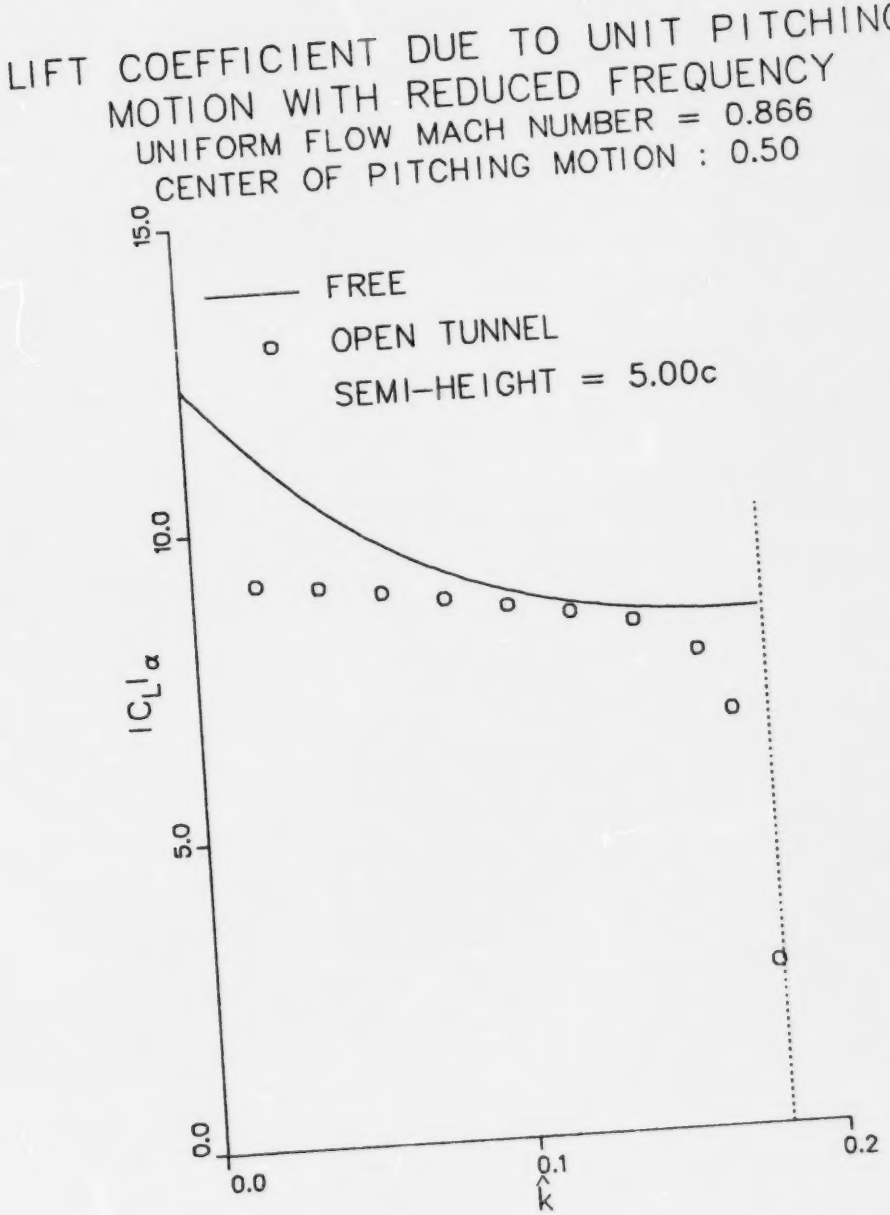

FIG. 9: $|C_L|_\alpha$ vs $\hat{k}$

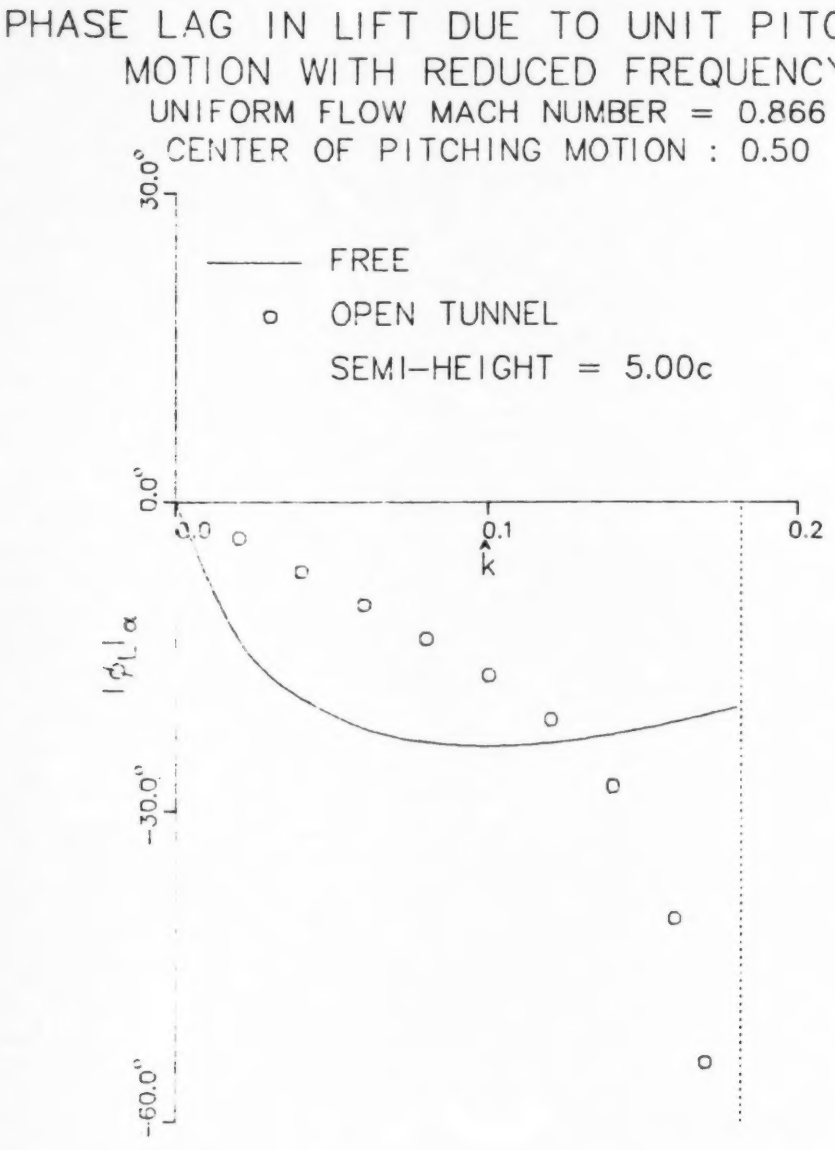

FIG. 10: $|\phi_L|_\alpha$ **vs** $\hat{k}$

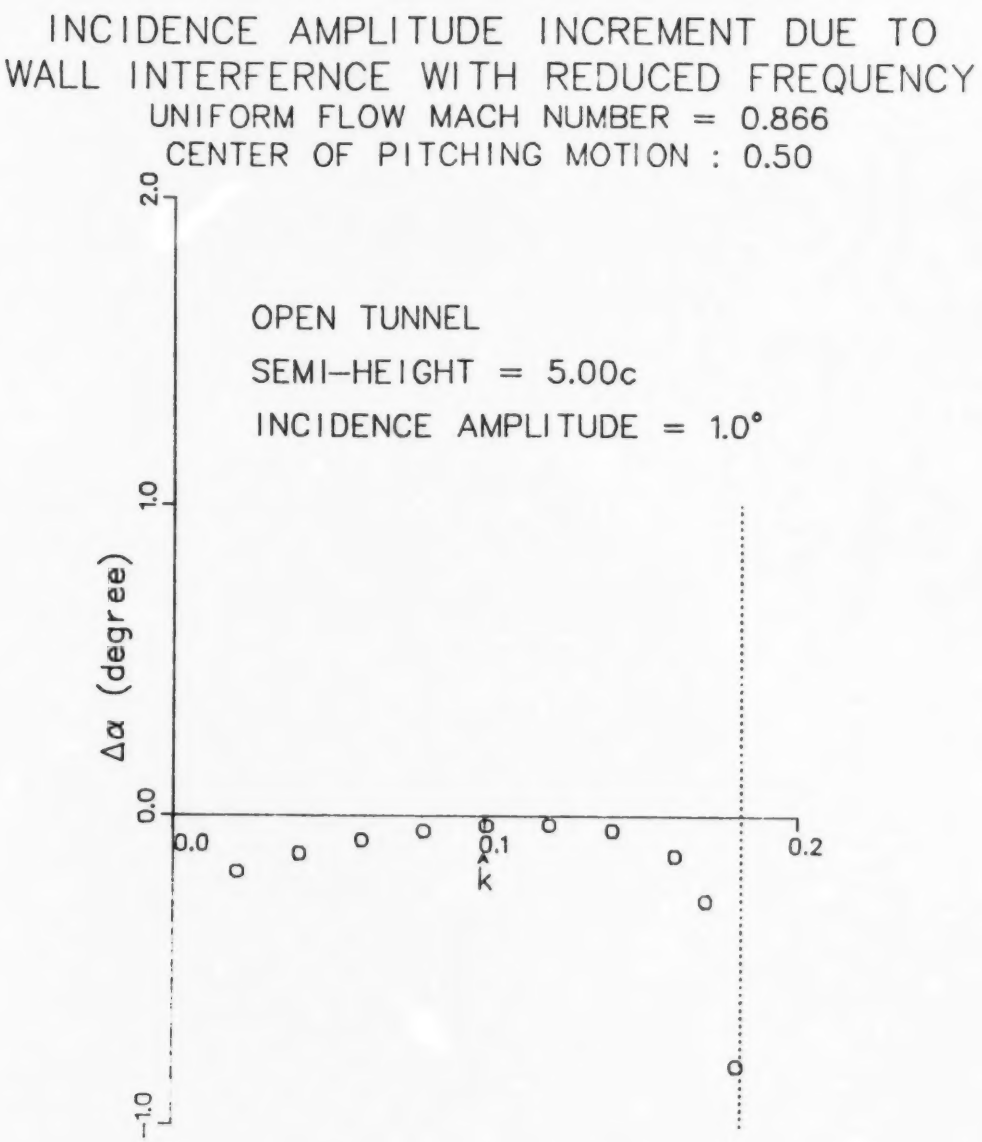

FIG. 11: $\Delta\alpha_A$ **vs** $\hat{k}$

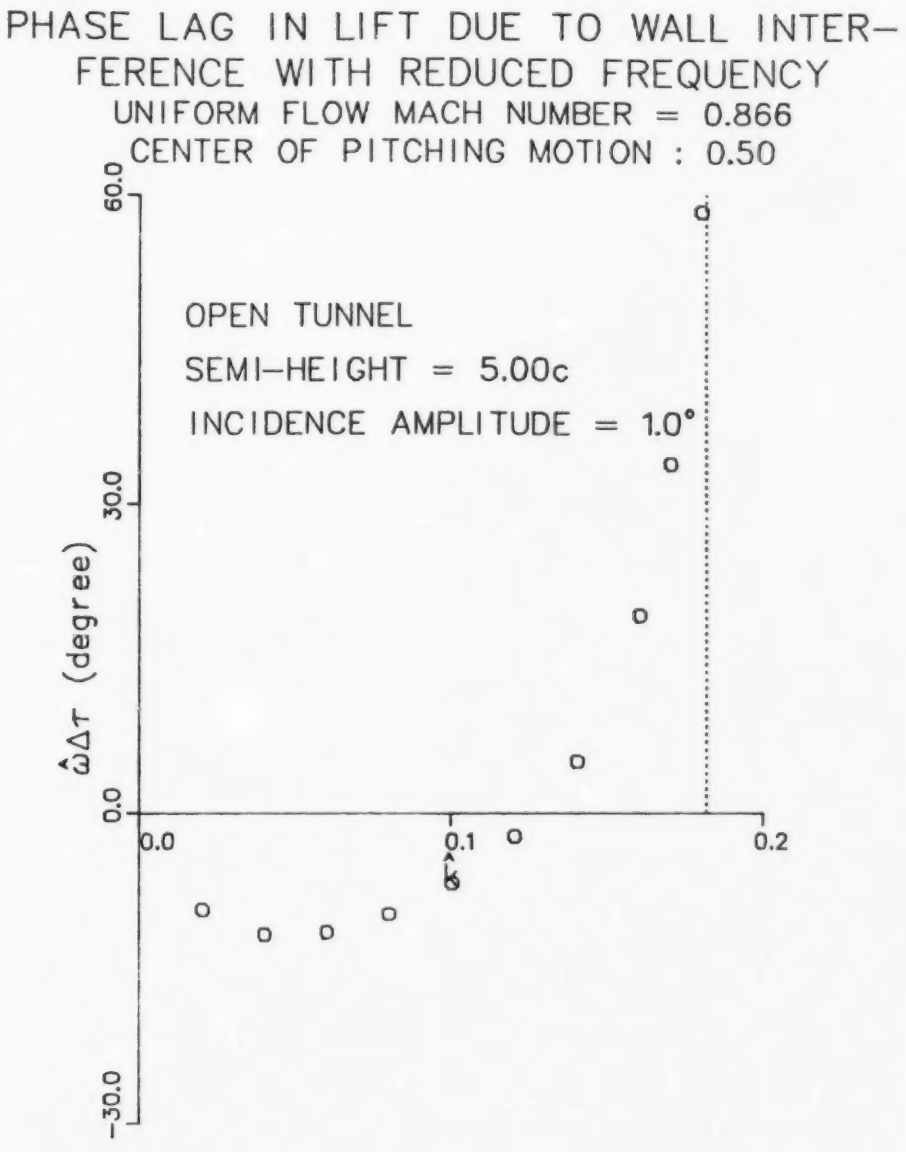

FIG. 12: $\omega\Delta\tau$ **vs** $\hat{k}$

PRESSURE DIFFERENCE DISTRIBUTION

$$\Delta C_{PC}\cos(\hat{\omega}\hat{t})+\Delta C_{PS}\sin(\hat{\omega}\hat{t})$$

UNIFORM MACH NUMBER = 0.866

REDUCED FREQUENCY = 0.080

THE CENTER OF PITCHING : 0.50

—— ΔC_{pc} IN FREE AIR

..... ΔC_{ps} IN FREE AIR $\alpha_A = 0.951^0$

× OPEN TUNNEL $\hat{h}/c = 5.00$ $\alpha_A = 1.000^0$

o CORRECTED $\alpha_A = 0.951^0$

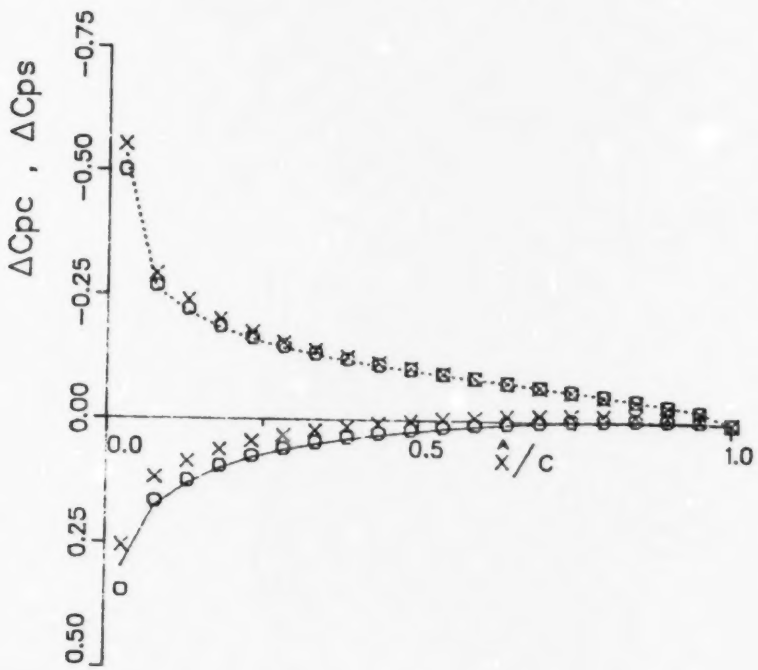

FIG. 13: ΔC_p vs $\hat{x}/c$

PRESSURE DIFFERENCE DISTRIBUTION

$\Delta C_{PC}\cos(\hat{\omega}\hat{t})+\Delta C_{PS}\sin(\hat{\omega}\hat{t})$

UNIFORM MACH NUMBER = 0.866

REDUCED FREQUENCY = 0.170

THE CENTER OF PITCHING : 0.50

—— ΔC_{pc} IN FREE AIR

..... ΔC_{ps} IN FREE AIR $\alpha_A = 0.724°$

× OPEN TUNNEL $\hat{H}/c = 5.00$ $\alpha_A = 1.000°$

o CORRECTED $\alpha_A = 0.724°$

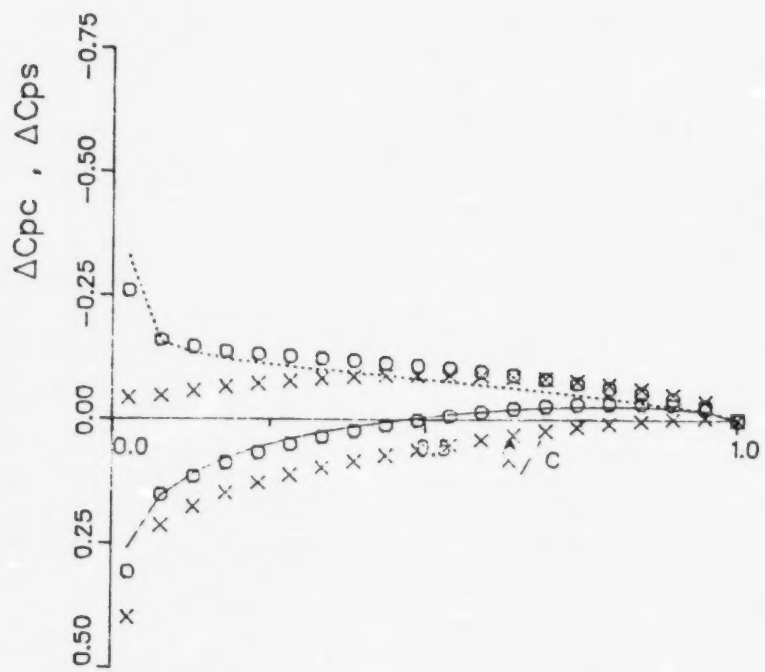

FIG. 14: ΔC_p vs $\hat{x}/c$

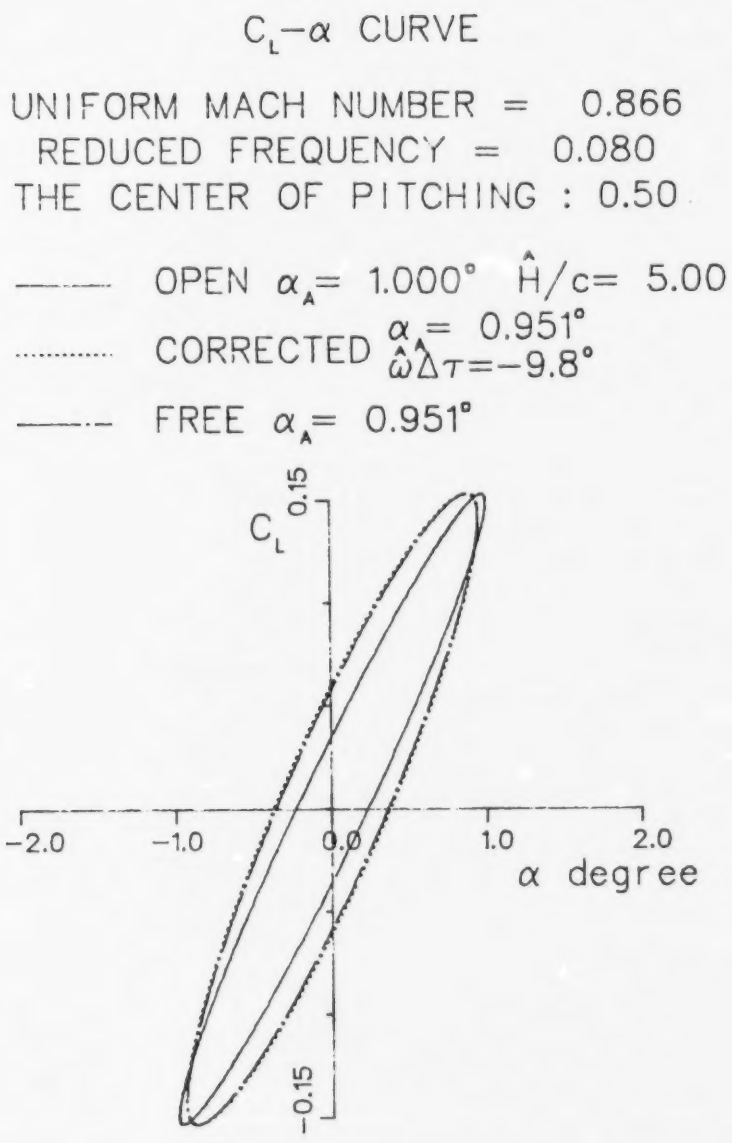
$C_L-\alpha$ CURVE
UNIFORM MACH NUMBER = 0.866
REDUCED FREQUENCY = 0.080
THE CENTER OF PITCHING : 0.50
OPEN α_A= 1.000° $\hat{H}/c$= 5.00
CORRECTED α_A= 0.951°
$\hat{\omega}\Delta\tau$=−9.8°
FREE α_A= 0.951°
C_L
0.15
−0.15
−2.0
−1.0
0.0
1.0
2.0
α degree

FIG. 15: C_L vs α

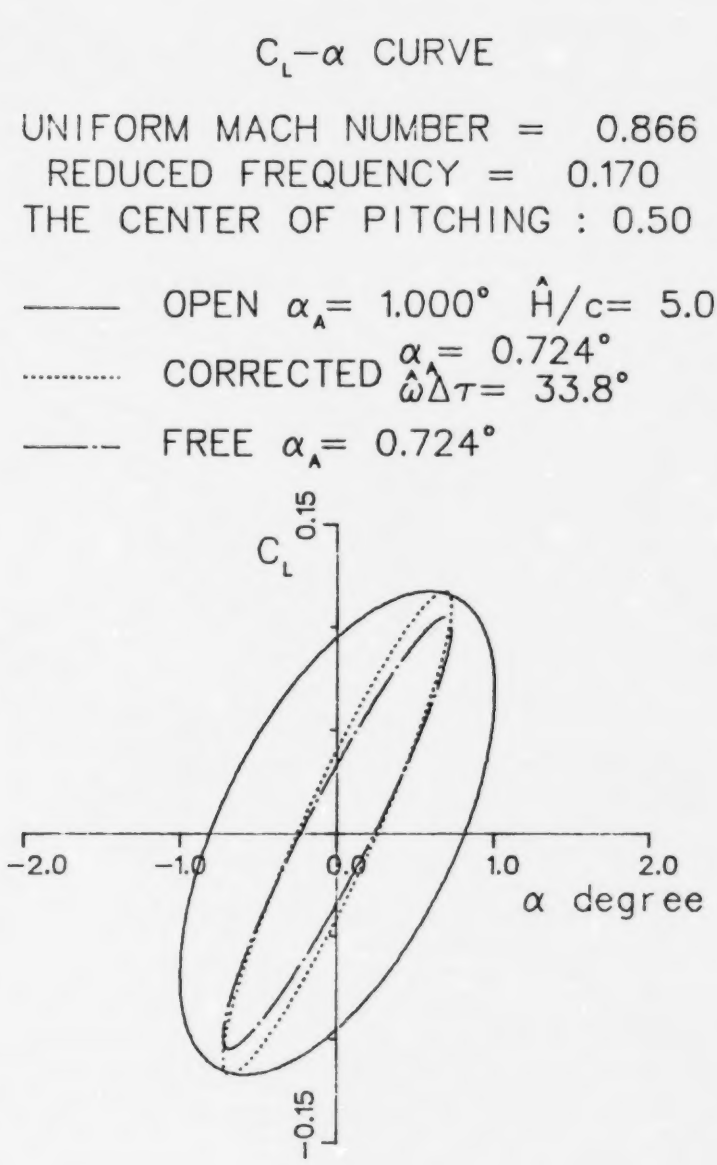

FIG. 16: C_L vs α

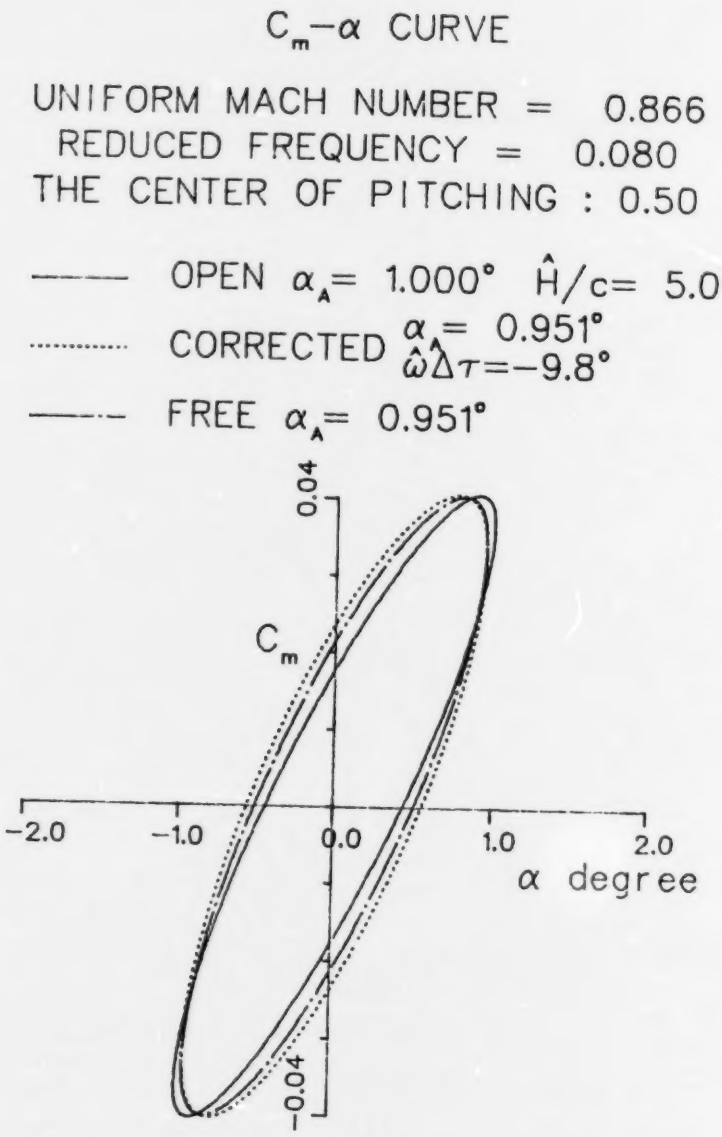

FIG. 17: C_m vs α

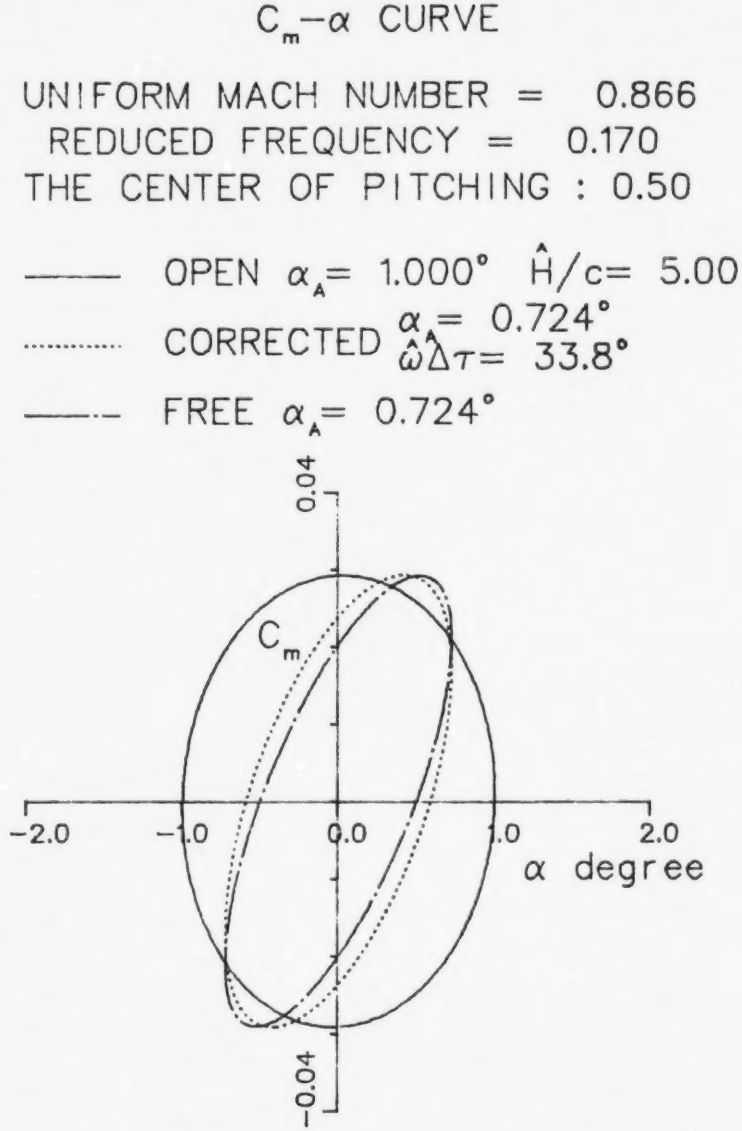

FIG. 18: C_m vs α

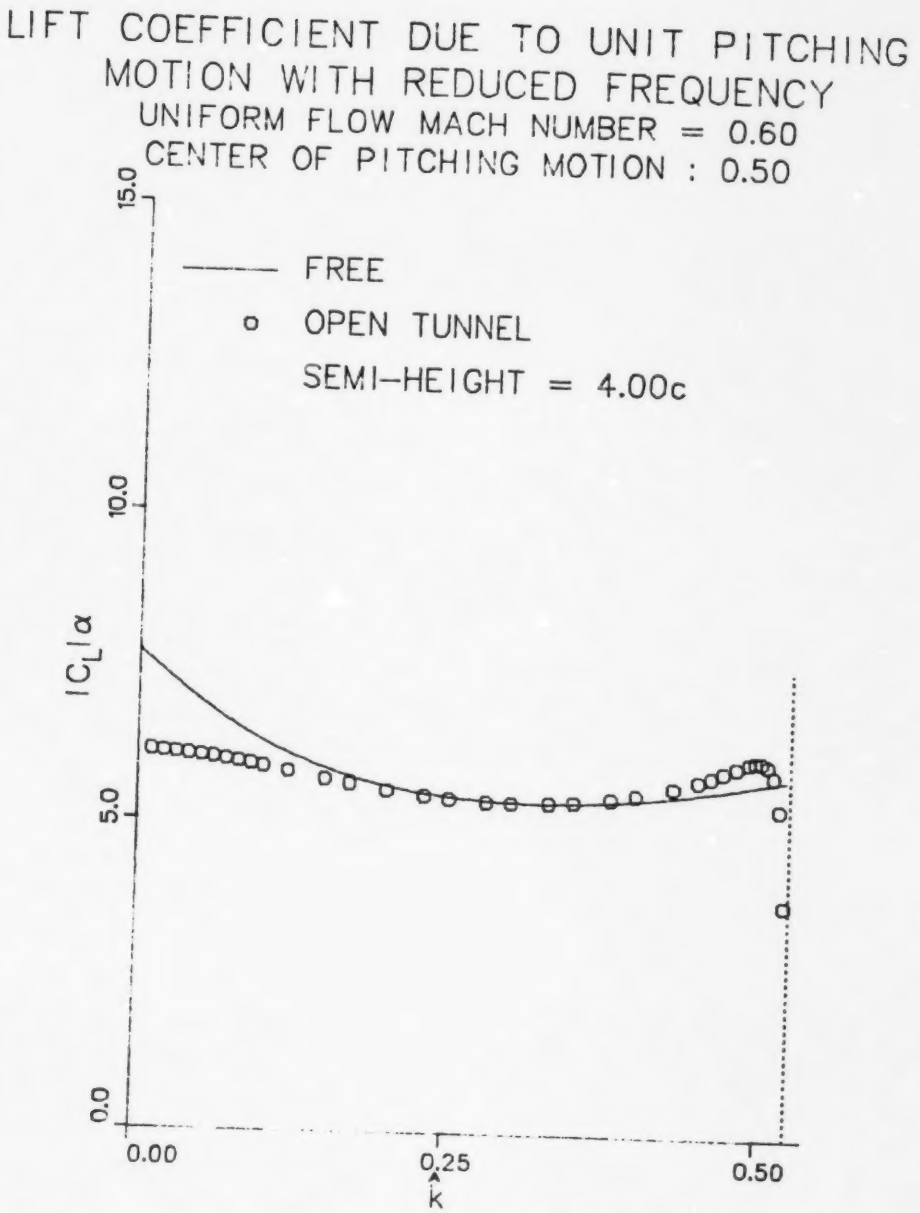

FIG. 19: $|C_L|_\alpha$ **vs** $\hat{k}$

PHASE LAG IN LIFT DUE TO UNIT PITCHING MOTION WITH REDUCED FREQUENCY
UNIFORM FLOW MACH NUMBER = 0.60
CENTER OF PITCHING MOTION : 0.50

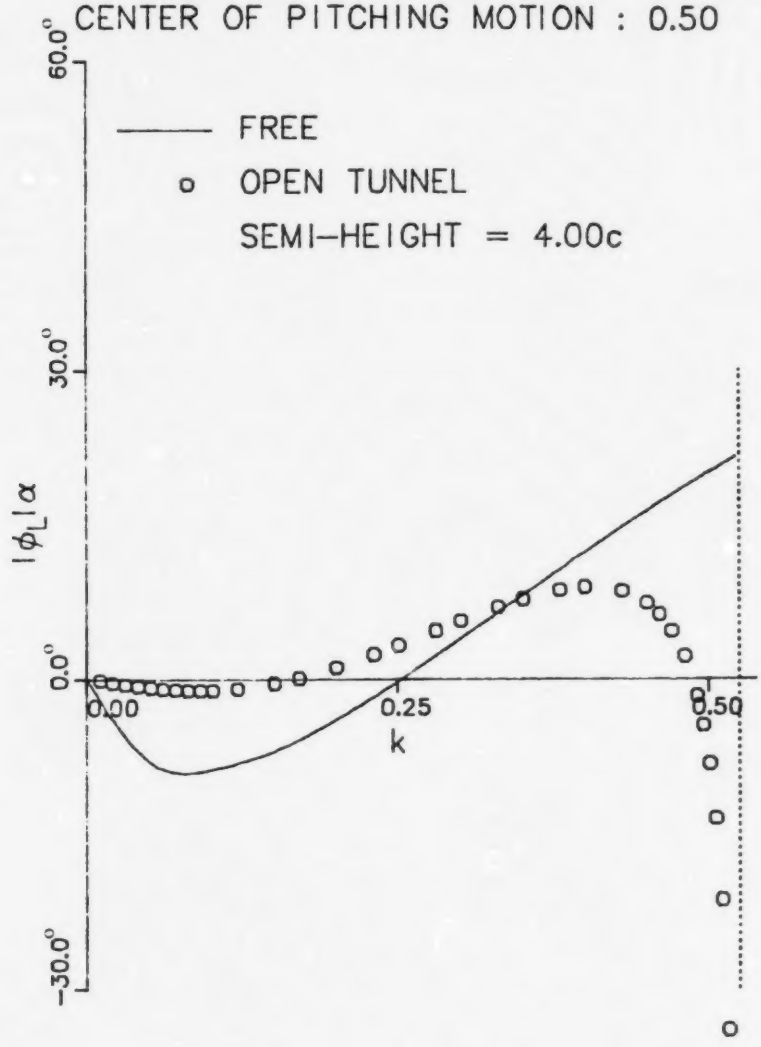

FIG. 20: $|\phi_L|_\alpha$ vs $\hat{k}$

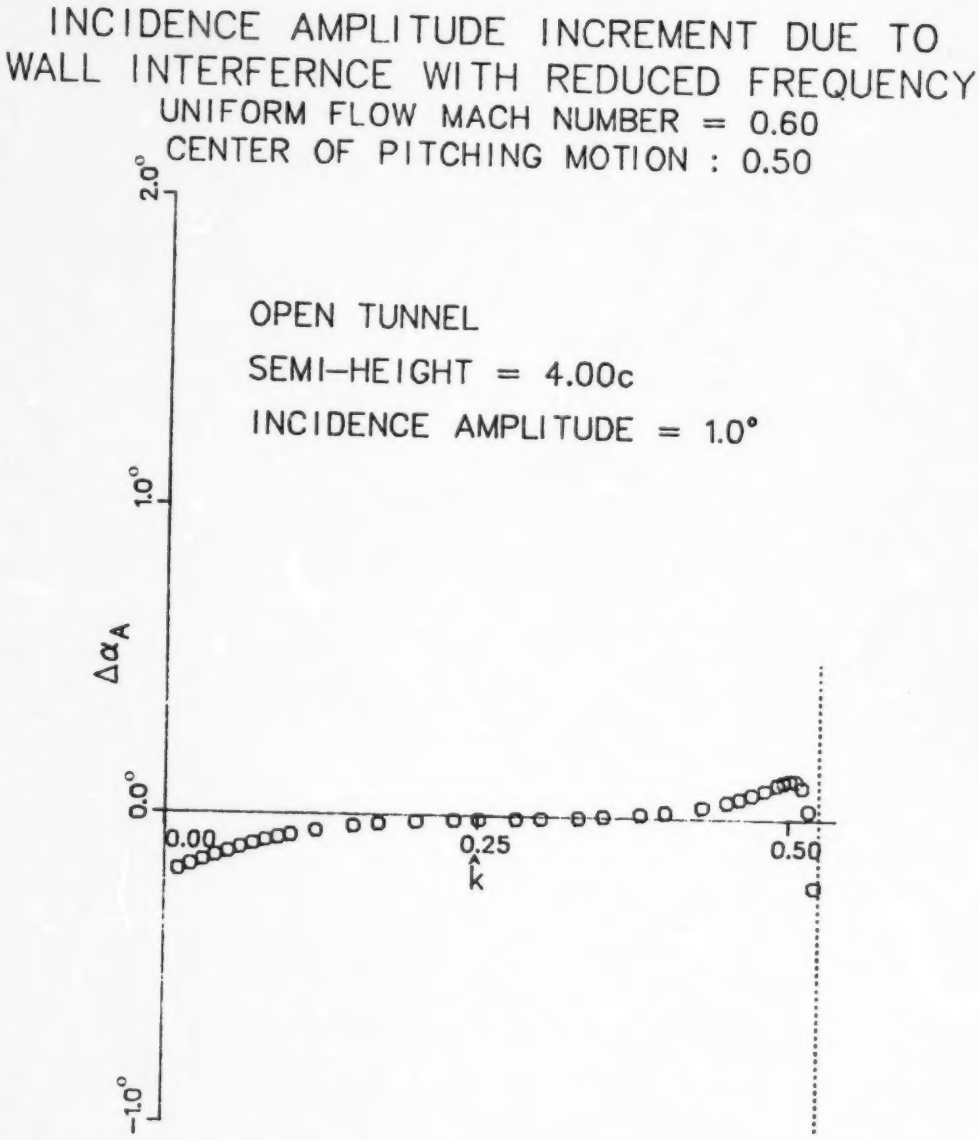

FIG. 21: $\Delta\alpha_A$ **vs** $\hat{k}$

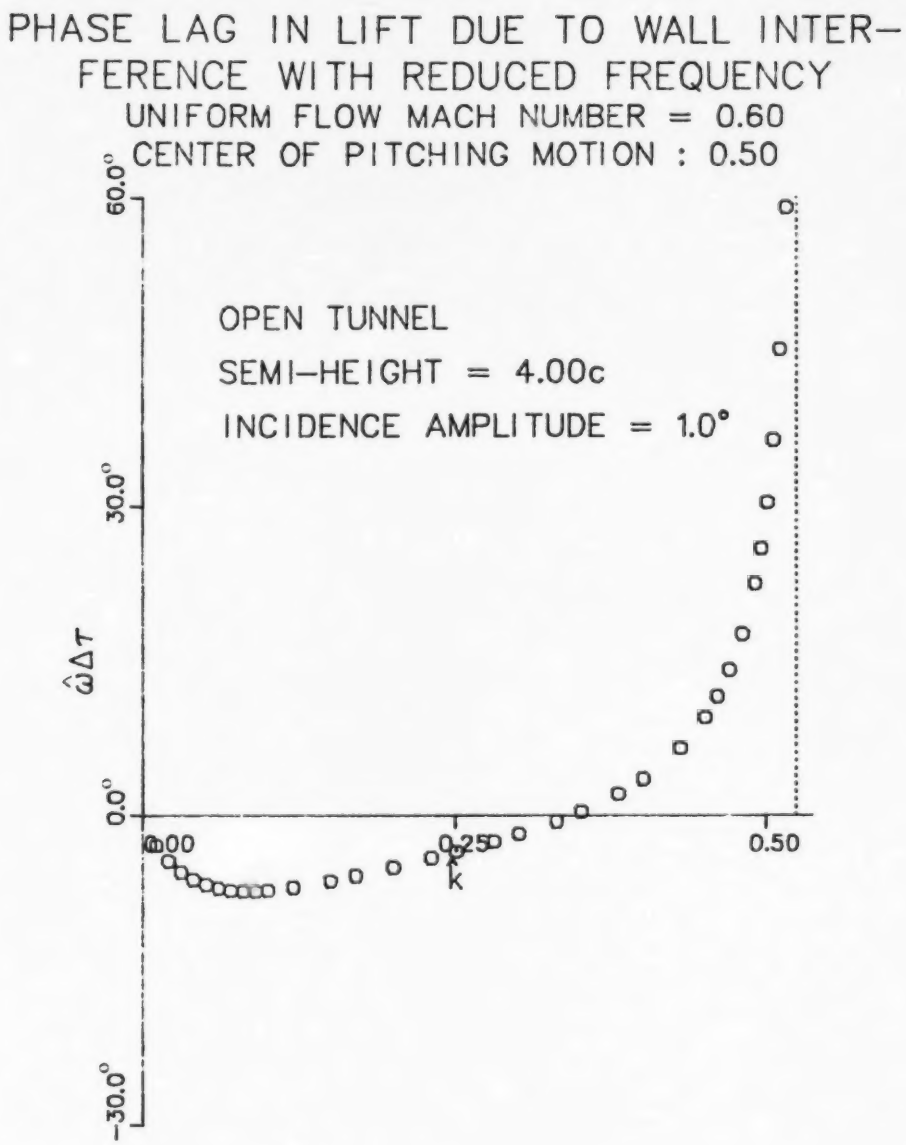

FIG. 22: $\omega\Delta\tau$ **vs** $\hat{k}$

PRESSURE DIFFERENCE DISTRIBUTION

$\Delta C_{PC}\cos(\hat{\omega}\hat{t})+\Delta C_{PS}\sin(\hat{\omega}\hat{t})$

UNIFORM MACH NUMBER = 0.600

REDUCED FREQUENCY = 0.100

THE CENTER OF PITCHING : 0.50

—— ΔC_{pc} IN FREE AIR

····· ΔC_{ps} IN FREE AIR $\alpha_A = 0.931^\circ$

× OPEN TUNNEL $\hat{H}/c = 4.00$ $\alpha_A = 1.000^\circ$

o CORRECTED $\alpha_A = 0.931^\circ$

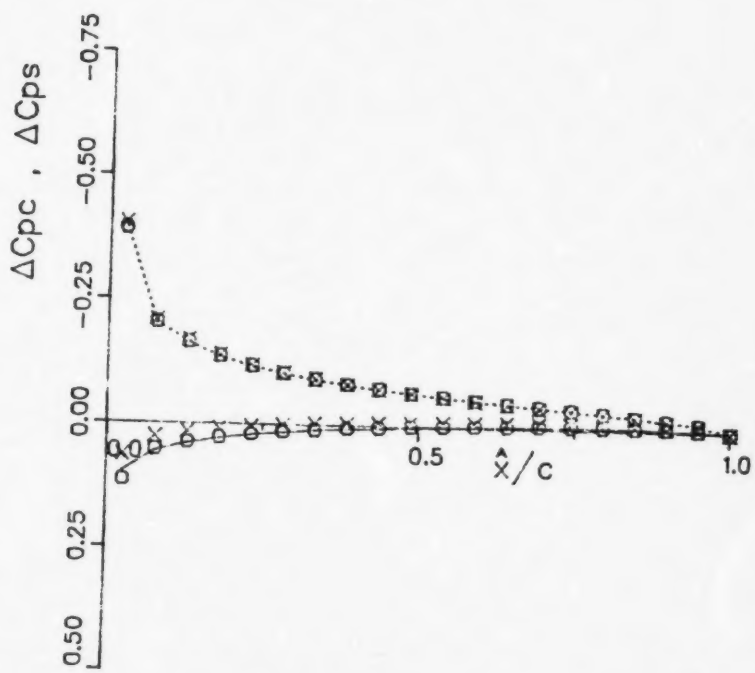

FIG. 23: ΔC_p vs $\hat{x}/c$

PRESSURE DIFFERENCE DISTRIBUTION

$$\Delta C_{PC}\cos(\hat{\omega}\hat{t})+\Delta C_{PS}\sin(\hat{\omega}\hat{t})$$

UNIFORM MACH NUMBER = 0.600
REDUCED FREQUENCY = 0.500
THE CENTER OF PITCHING : 0.50

—— ΔC_{pc} IN FREE AIR $\alpha_A = 1.126^\circ$
..... ΔC_{ps} IN FREE AIR
× OPEN TUNNEL $\hat{H}/c = 4.00$ $\alpha_A = 1.000^\circ$
o CORRECTED $\alpha_A = 1.126^\circ$

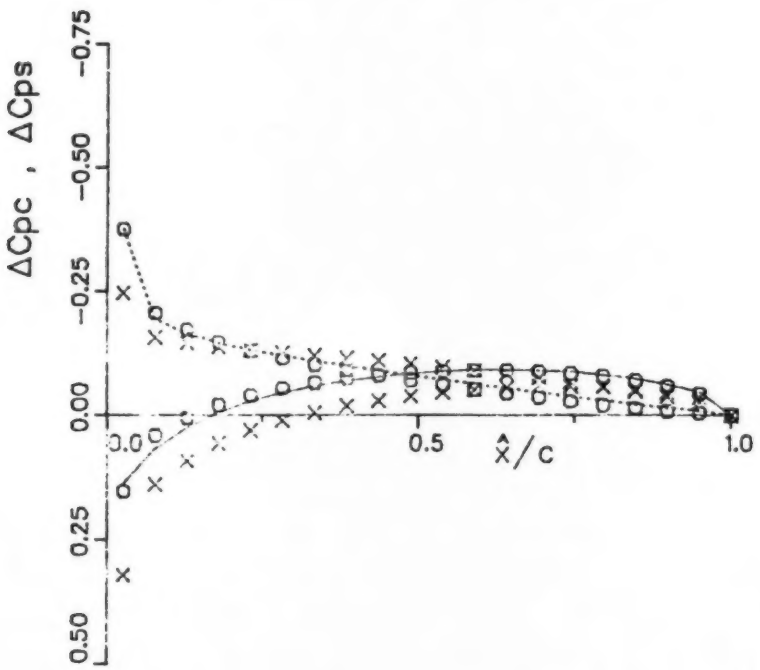

FIG. 24: ΔC_p vs $\hat{x}/c$

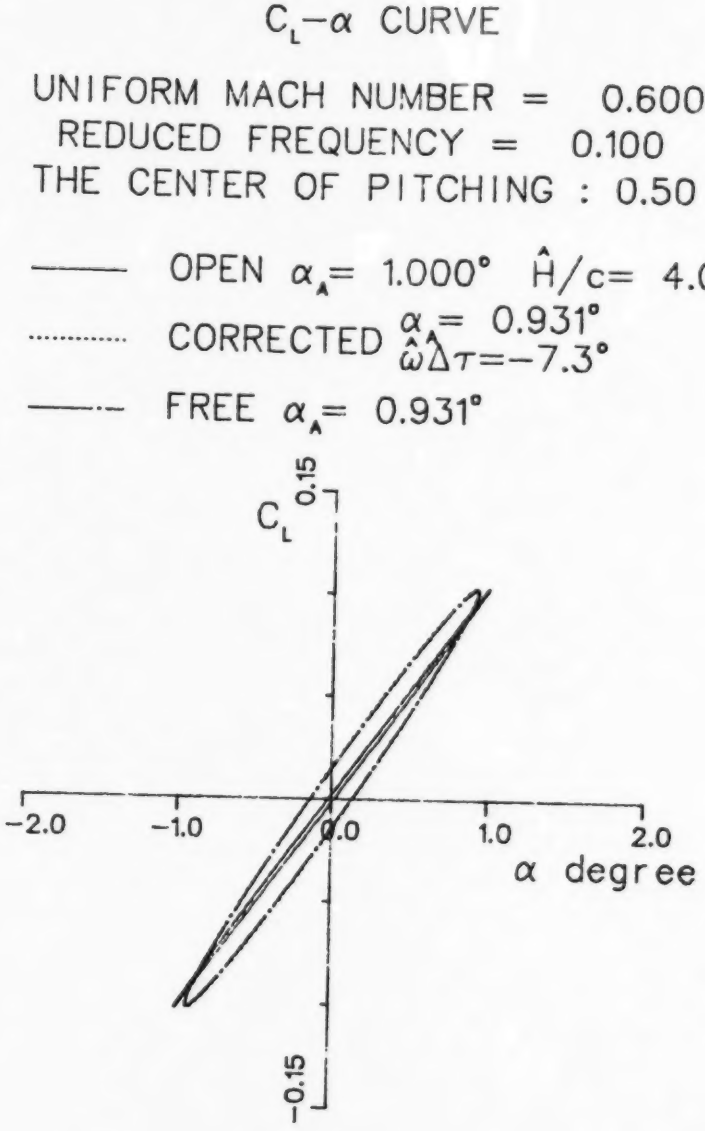

FIG. 25: C_L vs α

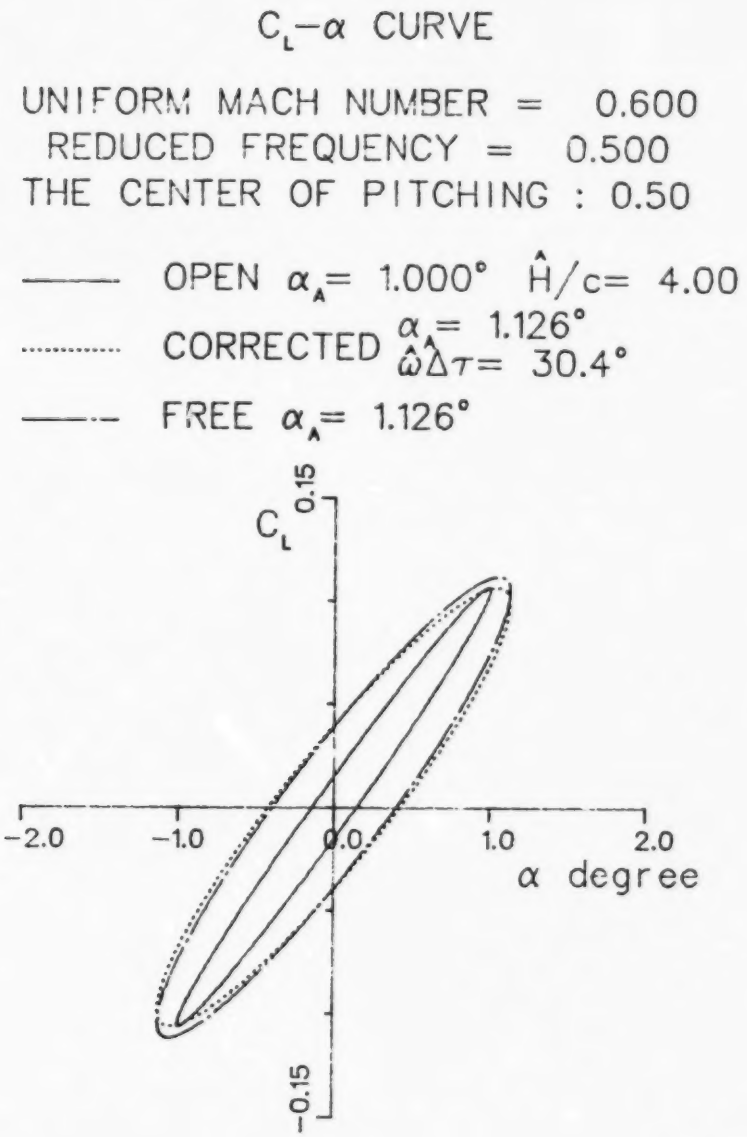

FIG. 26: C_L vs α

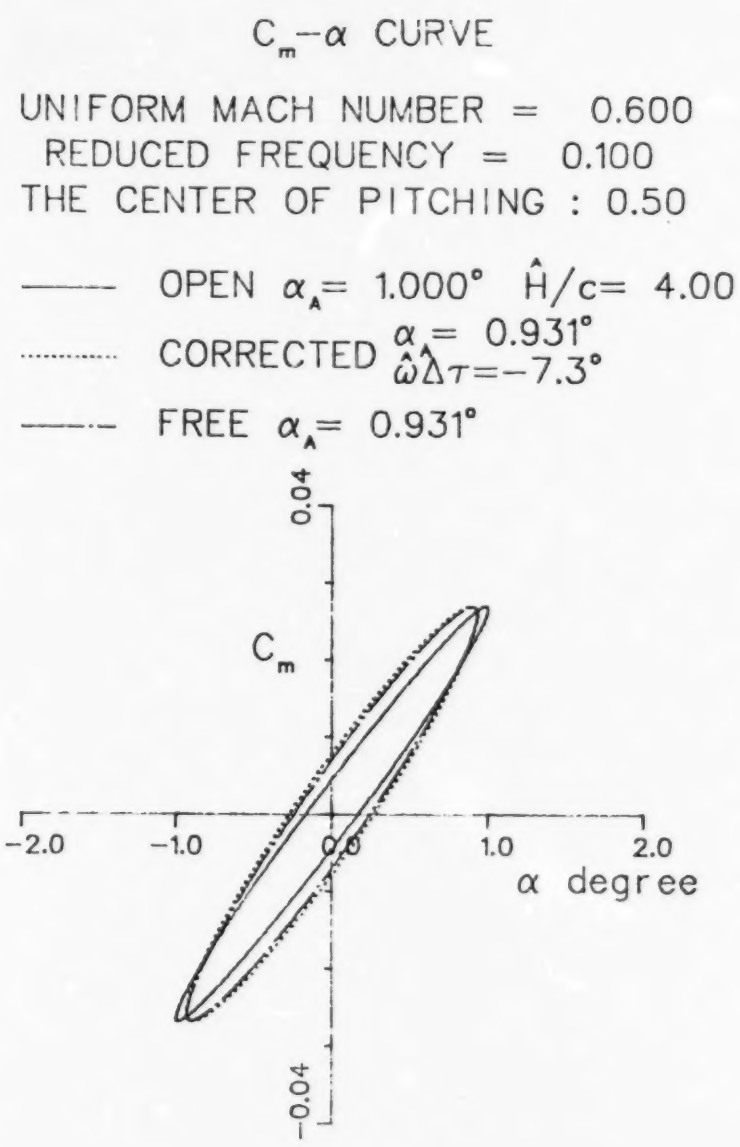

FIG. 27: C_m vs α

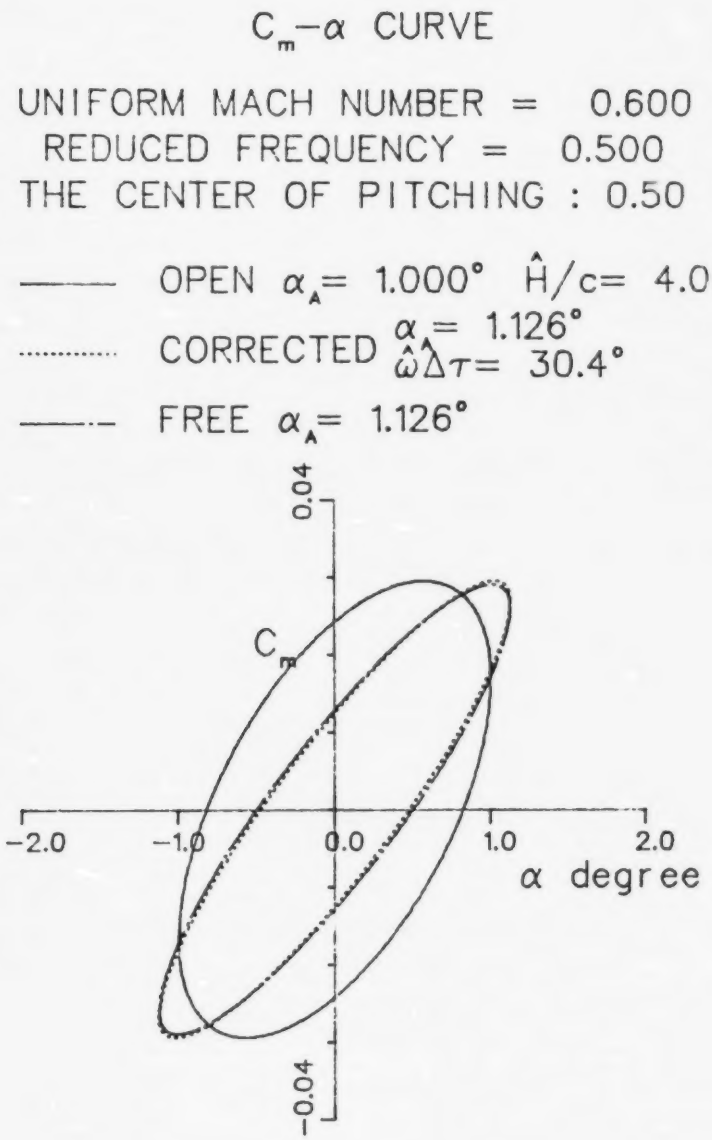

FIG. 28: C_m vs α

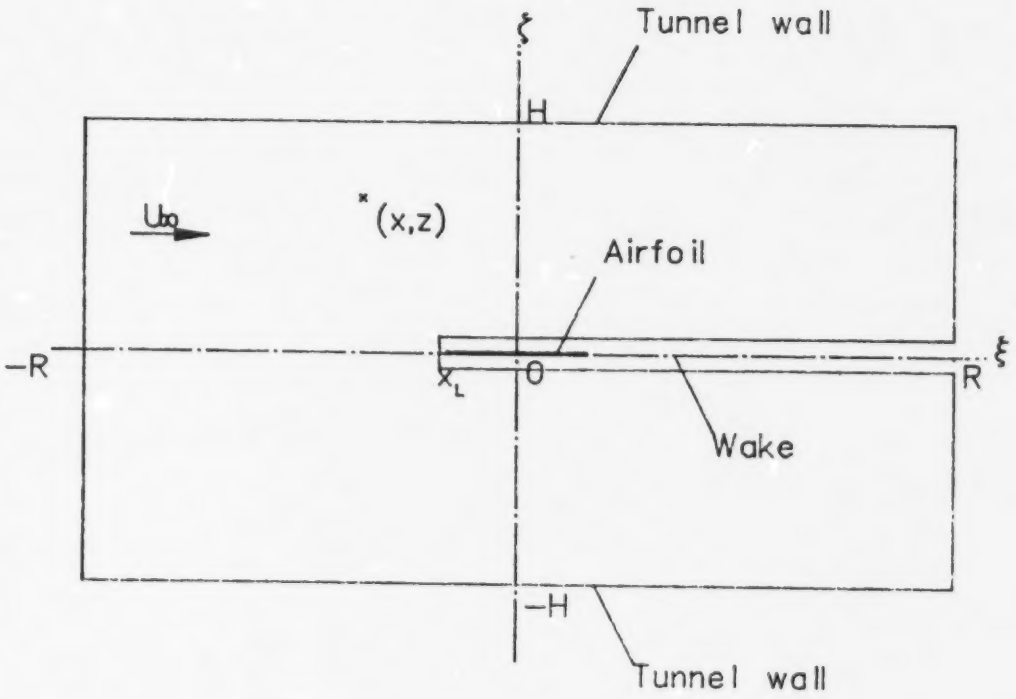

FIG. 29: DOMAIN OF FLOW FIELD IN A TUNNEL

APPENDIX A

DERIVATION OF EQUATION (19)

Firstly it will be proved that $\widetilde{\psi}(\xi,\zeta;x,z)$ in Equation (17) satisfies the Helmoltz equation Equation (18) everywhere except at a point (x,z). Equation (19) will be obtained later.

$\widetilde{\psi}(\xi,\zeta;x,z)$ in Equation (17) is bounded everywhere except at a point (x,z). Unless $\zeta = z$, the derivative of $\widetilde{\psi}$ with ξ or ζ can be obtained by the way of differentiating the two integrands on the right-hand side of Equation (17) directly with ξ or ζ. So $\widetilde{\psi}$ satisfies Equation (18) unless $\zeta = z$. From Equation (17) it follows:

$$\left.\frac{\partial\widetilde{\psi}}{\partial\zeta}\right|_{\zeta\neq z} = \frac{\kappa}{2\pi}\cdot \mathrm{sgn}(\zeta-z)\cdot\left\{\int_0^1 \cos\{\kappa|\zeta-z|\sqrt{1-\theta^2}\}\cdot\cos\{\kappa(\xi-x)\theta\}\,d\theta + \int_1^\infty e^{-\kappa|\zeta-z|\sqrt{\theta^2-1}}\cdot\cos\{\kappa(\xi-x)\theta\}\,d\theta\right\}. \tag{A-1}$$

Equation (A-1) can be arranged to give:

$$\begin{aligned}\left.\frac{\partial\widetilde{\psi}}{\partial\zeta}\right|_{\zeta\neq z} = \frac{\kappa}{2\pi}\cdot\mathrm{sgn}(\zeta-z)\cdot\Big[&\int_0^1\cos\{\kappa(\xi-x)\theta\}\,d\theta + \int_1^\infty e^{-\kappa|\zeta-z|\theta}\cdot\cos\{\kappa(\xi-x)\theta\}\,d\theta\\ &-\int_0^1\left\{1-\cos\{\kappa|\zeta-z|\sqrt{1-\theta^2}\}\right\}\cdot\cos\{\kappa(\xi-x)\cdot\theta\}\,d\theta\\ &-\int_1^\infty\left\{e^{-\kappa|\zeta-z|\theta}-e^{-\kappa|\zeta-z|\sqrt{\theta^2-1}}\right\}\cdot\cos\{\kappa(\xi-x)\cdot\theta\}\,d\theta\Big].\end{aligned} \tag{A-2}$$

Because the first two integrals at the right-hand side of Equation (A-2) can be estimated analytically easily, Equation (A-2) reduces to

$$\begin{aligned}\left.\frac{\partial\widetilde{\psi}}{\partial\zeta}\right|_{\zeta\neq z} = \frac{\kappa}{2\pi}\cdot\mathrm{sgn}(\zeta-z)\cdot\Big[&\frac{1}{\kappa(\xi-x)}\cdot\sin\{\kappa(\xi-x)\} - \frac{1}{\kappa}\cdot\frac{\xi-x}{(\xi-x)^2+(\zeta-z)^2}\cdot\sin\{\kappa(\xi-x)\}\\ &-\frac{1}{\kappa}\cdot\frac{|\zeta-z|}{(\xi-x)^2+(\zeta-z)^2}\cdot\cos\{\kappa(\xi-x)\}\\ &-\int_0^1\left\{1-\cos(\kappa|\zeta-z|\sqrt{1-\theta^2})\right\}\cdot\cos\{\kappa(\xi-x)\}\,d\theta\\ &-\int_1^\infty\left\{e^{-\kappa|\zeta-z|\theta}-e^{-\kappa|\zeta-z|\sqrt{\theta^2-1}}\right\}\cdot\cos\{\kappa(\xi-x)\}\,d\theta\Big]\quad;\ \xi\neq x.\end{aligned} \tag{A-2a}$$

So

$$\lim_{\zeta\to z+0}\frac{\partial\widetilde{\psi}}{\partial\zeta} = \lim_{\zeta\to z-0}\frac{\partial\widetilde{\psi}}{\partial\zeta} = 0\quad;\quad \xi\neq x. \tag{A-3}$$

Because $\widetilde{\psi}$ is continuous with ζ except at a point (x,z) and because of the relation (A-3), the derivative of $\widetilde{\psi}$ with ζ on the line $\zeta = z$ exists and its value is also 0 unless $\xi \neq x$. The derivative of $\widetilde{\psi}$ with ζ is also continuous with respect to ζ except at a point (x,z). The second derivative of $\widetilde{\psi}$ with ζ is obtained from Equation (18):

$$\begin{aligned}\left.\frac{\partial^2\widetilde{\psi}}{\partial\zeta^2}\right|_{\zeta\neq z} = &-\frac{\kappa}{2\pi}\int_0^1\sqrt{1-\theta^2}\cdot\sin\{\kappa|\zeta-z|\sqrt{1-\theta^2}\}\cdot\cos\{\kappa(\xi-x)\theta\}\,d\theta\\ &-\frac{\kappa}{2\pi}\int_1^\infty\sqrt{\theta^2-1}\cdot e^{-\kappa|\zeta-z|\sqrt{\theta^2-1}}\cdot\cos\{\kappa(\xi-x)\theta\}\,d\theta.\end{aligned} \tag{A-4}$$

From Equation (A-4), the second derivative is symmetric with respect to $(\zeta - z)$. Resultantly the second derivative does exist and its value is

$$\left.\frac{\partial^2 \tilde{\psi}}{\partial \zeta^2}\right|_{\zeta=z} = \lim_{\zeta \to z \pm 0} \left.\frac{\partial^2 \tilde{\psi}}{\partial \zeta^2}\right|_{\zeta \neq z} \quad ; \ \xi \neq x, \tag{A-5}$$

because of the same reason as the first derivative is estimated. From Equation (18), follows

$$\left.\tilde{\psi}\right|_{\zeta=z} = \frac{1}{4} N_0(\kappa|\xi - x|) , \tag{A-6}$$

where N_0 is the Newmann function. So the first and second derivatives with ξ exist unless $\xi = x$. Because the second derivative of $\tilde{\psi}$ with ξ at $\zeta \neq z$ is symmetric with respect to $(\zeta - z)$,

$$\left.\frac{\partial^2 \tilde{\psi}}{\partial \xi^2}\right|_{\zeta=z} = \lim_{\zeta \to z \pm 0} \left.\frac{\partial^2 \tilde{\psi}}{\partial \xi^2}\right|_{\zeta \neq z} . \tag{A-7}$$

It is of course that the second derivatives of $\tilde{\psi}$ with both ξ and ζ are bounded even if ζ tends to z unless $\xi = x$. Resultantly $\tilde{\psi}(\xi,\zeta;x,z)$ can satisfy Equation (18) everywhere except for a point (x,z).

Now suppose a small circle in the considered space (ξ,ζ) which has a radius ρ and its center at (x,z). An arbitrary point (ξ,ζ) on the circle can be expressed:

$$\begin{aligned} \xi &= x + \rho \cdot \cos\psi , \\ \zeta &= z + \rho \cdot \sin\psi \ ; \quad \rho > 0 . \end{aligned} \tag{A-8}$$

If n is the inward normal co-ordinate to the circle,

$$\frac{\partial \tilde{\psi}}{\partial n} = -\frac{\partial \tilde{\psi}}{\partial \rho} . \tag{A-9}$$

Therefore

$$\begin{aligned} \frac{\partial \tilde{\psi}}{\partial n} = &- \frac{\kappa}{2\pi} \cdot |\sin\psi| \cdot \int_1^\infty e^{-\kappa\rho|\sin\psi|\sqrt{\theta^2-1}} \cdot \cos\{\kappa\rho(\cos\psi)\theta\}\, d\theta \\ &- \frac{\kappa}{2\pi} \cdot \cos\psi \cdot \int_1^\infty \frac{\theta}{\sqrt{\theta^2-1}} \cdot e^{-\kappa\rho|\sin\psi|\sqrt{\theta^2-1}} \cdot \sin\{\kappa\rho(\cos\psi)\theta\}\, d\theta \\ &+ P(\rho,\psi) , \end{aligned} \tag{A-10}$$

where P is bounded for both ρ and ψ. This circle is notated with $\partial\Omega\rho$.

$$\oint_{\partial\Omega\rho} \frac{\partial \tilde{\psi}}{\partial n} \cdot \tilde{\phi}^* \, ds = -\tilde{\phi}^*(x_0, z_0) \cdot \rho \int_0^{2\pi} \frac{\partial \tilde{\psi}}{\partial \rho} \, d\psi , \tag{A-11}$$

where (x_0, z_0) is in $\partial\Omega\rho$.

$$\lim_{\rho \to 0} \rho \int_0^{2\pi} \frac{\partial \tilde{\psi}}{\partial \rho} \, d\psi = 1 . \tag{A-12}$$

Because

$$\lim_{\rho \to 0} \rho \int_0^{2\pi} P(\rho,\psi) \, d\psi = 0 , \tag{A-13}$$

$$\lim_{\rho\to 0}\ \rho\int_0^{2\pi}\left[\frac{\kappa}{2\pi}\cdot|\sin\psi|\cdot\int_1^{\infty} e^{-\kappa\rho|\sin\psi|\sqrt{\theta^2-1}}\cdot\cos\{\kappa\rho(\cos\psi)\theta\}\,d\theta\right]d\psi\ =\ \frac{1}{2\pi}\int_0^{2\pi}\sin^2\psi\,d\psi\ , \qquad \text{(A-14)}$$

and

$$\lim_{\rho\to 0}\ \rho\int_0^{2\pi}\left[\frac{\kappa}{2\pi}\cdot\cos\psi\cdot\int_1^{\infty}\frac{\theta}{\sqrt{\theta^2-1}}\cdot e^{-\kappa\rho|\sin\psi|\sqrt{\theta^2-1}}\cdot\sin\{\kappa\rho(\cos\psi)\theta\}\,d\theta\right]d\psi=\frac{1}{2\pi}\int_0^{2\pi}\cos^2\psi\,d\psi\ . \qquad \text{(A-15)}$$

Then

$$\lim_{\rho\to 0}\ \oint_{\partial\Omega_\rho}\frac{\partial\tilde{\psi}}{\partial n}\cdot\tilde{\phi}^*\,ds\ =\ -\,\tilde{\phi}^*(x,z)\ . \qquad \text{(A-16)}$$

Similarly $\tilde{\psi}$ on the circle is

$$\tilde{\psi}=-\frac{1}{2\pi}\int_1^{\infty}\frac{1}{\sqrt{\theta^2-1}}\cdot e^{-\rho\kappa|\sin\psi|\sqrt{\theta^2-1}}\cdot\cos\{\kappa\rho(\cos\psi)\theta\}\,d\theta+Q(\rho,\psi)\ , \qquad \text{(A-17)}$$

where $Q(\rho,\psi)$ is bounded for both ρ and ψ. Then

$$\left|\oint_{\partial\Omega_\rho}\tilde{\psi}\cdot\frac{\partial\tilde{\phi}^*}{\partial n}\,ds\right|\ \le\ \rho M\cdot\left|\int_0^{2\pi}\tilde{\psi}\,d\psi\right|\ , \qquad \text{(A-18)}$$

where M is the maximum value of $\partial\phi^*/\partial n$ on $\partial\Omega\rho$. From Equation (A-17) follows

$$|\tilde{\psi}|\ \le\ \frac{1}{2\pi}\left|\int_1^{\infty}\frac{1}{\sqrt{\theta^2-1}}\cdot e^{-\rho\kappa|\sin\psi|\sqrt{\theta^2-1}}\cdot\cos\{\kappa\rho(\cos\psi)\theta\}\,d\theta\right|+|Q|\ . \qquad \text{(A-19)}$$

The integral at the right-hand side of Equation (A-19) reduces to

$$\frac{1}{2\pi}\left|\int_1^{\infty}\frac{1}{\sqrt{\theta^2-1}}\cdot e^{-\rho\kappa|\sin\psi|\sqrt{\theta^2-1}}\cdot\cos\{\kappa\rho(\cos\psi)\theta\}\,d\theta\right|$$

$$\le\ \frac{1}{2\pi}\int_0^{\infty}\frac{1}{\sqrt{\vartheta^2+1}}\cdot e^{-\rho\kappa|\sin\psi|\cdot\vartheta}\cdot d\vartheta\ =\ \frac{1}{4}\{H_0(\kappa\rho|\sin\psi|)-N_0(\kappa\rho|\sin\psi|)\}\ , \qquad \text{(A-20)}$$

where H_0 is the Struve function and bounded for any value of its variable. The Newmann function N_0 has the following property:

$$N_0(x)\ =\ \frac{2}{\pi}\cdot J_0(x)\cdot\{\log\left(\frac{x}{2}\right)+\gamma\}$$

$$-\frac{2}{\pi}\sum_{k=0}^{\infty}\frac{(-1)^k}{(k!)^2}\cdot\left(\frac{x}{2}\right)^{2k}\cdot\sum_{m=1}^{k}\frac{1}{m}\ , \qquad \text{(A-21)}$$

where J_0 is the Bassel function and bounded for x and γ is the Euler constant number. (γ = 0.57721...) Then

$$\lim_{\rho\to 0}\ \rho\cdot|\tilde{\psi}|\ =\ 0\ . \qquad \text{(A-22)}$$

Resultantly from Equation (A-18) follows

$$\left| \oint_{\partial\Omega_\rho} \tilde{\psi} \cdot \frac{\partial \tilde{\Phi}^*}{\partial n} ds \right| \longrightarrow 0 \quad ; \quad \rho \longrightarrow 0 \quad . \tag{A-23}$$

With the aid of the thin airfoil approximation Equation (16) becomes

$$\tilde{\Phi}^*(x,z) = -\int_{x_L}^{\infty} \left[\tilde{\Phi}^* \cdot \frac{\partial \tilde{\psi}}{\partial \zeta} - \tilde{\psi} \cdot \frac{\partial \tilde{\Phi}^*}{\partial \zeta} \right]_-^+ d\xi + \oint_{\partial\Omega_R} \left(\tilde{\Phi}^* \cdot \frac{\partial \tilde{\psi}}{\partial n} - \tilde{\psi} \cdot \frac{\partial \tilde{\Phi}^*}{\partial n} \right) ds \ , \tag{A-24}$$

where $\partial\Omega_R$ is a circle with the radius R and its center at (x,z). As previously mentioned, $\tilde{\psi}$ and its first derivative with ζ are continuous except for a point (x,z). So the first integral becomes

$$-\int_{x_L}^{\infty} \left[\tilde{\Phi}^* \right]_-^+ \cdot \frac{\partial \tilde{\psi}}{\partial \zeta}\Big|_{\zeta=0} d\xi + \int_{x_L}^{\infty} \left[\frac{\partial \tilde{\Phi}^*}{\partial \zeta} \right]_-^+ \cdot \tilde{\psi}|_{\zeta=0} \, d\xi \ . \tag{A-25}$$

$\partial\phi^*/\partial\zeta$ means the upward velocity component and should be continuous throughout the flow field. But it must coincide with the vertical component of the airfoil surface velocity from x_L to x_T. x_L and x_T are the transformed leading and trailing edge co-ordinates, respectively. Because the airfoil model is oscillating in one piece, there is no difference in the vertical velocity between the upper and lower surfaces. Then

$$\left[\frac{\partial \tilde{\Phi}^*}{\partial \zeta} \right]_-^+ = 0 \quad ; \quad x \in [x_L, \infty) \ . \tag{A-26}$$

As a result the first integral of Equation (A-24) becomes

$$-\int_{x_L}^{\infty} \left[\tilde{\Phi}^* \right]_-^+ \cdot \frac{\partial \tilde{\psi}}{\partial \zeta}\Big|_{\zeta=0} d\xi \quad . \tag{A-27}$$

From Equations (A-10) and (A-17) it follows that

$$\left| \frac{\partial \tilde{\psi}}{\partial \rho}\Big|_{\rho=R} \right| = O\left(\frac{1}{\sqrt{R}}\right) \ ; \ [R \longrightarrow \infty] \ , \tag{A-28}$$

and

$$\left| \tilde{\psi}|_{\rho=R} \right| = O\left(\frac{1}{\sqrt{R}}\right) \ ; \ [R \longrightarrow \infty] \ , \tag{A-29}$$

where 'O' is the Landau's symbol and (A-28) means

$$\lim_{R\to\infty} \sqrt{R} \cdot \left| \frac{\partial \tilde{\psi}}{\partial \rho}|_{\rho=R} \right| = c \ . \tag{A-30}$$

Let

$$|\tilde{\Phi}^*|_{\rho=R} = O\left(\frac{1}{\sqrt{R}}\right) \ , \tag{A-31}$$

and

$$\left| \frac{\partial \tilde{\Phi}^*}{\partial \rho}\Big|_{\rho=R} \right| = O\left(\frac{1}{\sqrt{R}}\right) . \tag{A-32}$$

Then

$$\lim_{R\to\infty} R \cdot \left| \oint_{\partial\Omega_R} \left(\tilde{\Phi}^* \cdot \frac{\partial \tilde{\psi}}{\partial n} - \tilde{\psi} \cdot \frac{\partial \tilde{\Phi}^*}{\partial n} \right) ds \right| = 0 . \tag{A-33}$$

In this case Equation (A-24) becomes the same equation as Equation (19). However $\widetilde{CP}(\hat{x})$ obtained from the integral equation Equation (33) based on Equation (19) is limited because $\widetilde{\phi}^*$ corresponding to $\widetilde{CP}$ always satisfies the conditions (A-31 and (A-32). Experimentally such $\widetilde{CP}$ as is obtained from Equation (33) seems a good approximation for the flow considered. Both conditions (A-31) and (A-32) are assumed to be satisfied in this paper.

APPENDIX B

DERIVATION OF EQUATION (51)

The integral function on the right-hand side of Equation (47) is analytical everywhere including the point (x,z). The function also satisfy the Hermholtz equation Equation (50). As a result ψ is also a solution of Equation (50). Because ψ can be expressed in the form of the sum of $\widetilde{\psi}$ and an analytical function everywhere, Equation (46) reduces to the following form similarly to Equation (16): (see Fig. 29)

$$\begin{aligned}\phi^*(x,z) = &-\int_{-H}^{H}\left(\phi^*\cdot\frac{\partial\psi}{\partial\xi}-\psi\cdot\frac{\partial\phi^*}{\partial\xi}\right)\Big|_{\xi=-R}d\zeta\\ &+\int_{-H}^{H}\left(\phi^*\cdot\frac{\partial\psi}{\partial\xi}-\psi\cdot\frac{\partial\phi^*}{\partial\xi}\right)\Big|_{\xi=R}d\zeta\\ &+\int_{-R}^{R}\left[\phi^*\cdot\frac{\partial\psi}{\partial\zeta}-\psi\cdot\frac{\partial\phi^*}{\partial\zeta}\right]_{-H}^{H}d\xi\\ &-\int_{x_L}^{R}[\phi^*]_-^+\cdot\frac{\partial\psi}{\partial\zeta}\Big|_{\zeta=0}d\xi+\int_{x_L}^{R}\left[\frac{\partial\phi^*}{\partial\zeta}\right]_-^+\cdot\psi\Big|_{\zeta=0}d\xi\,.\end{aligned}\tag{B-1}$$

From the same reasoning as mentioned in Appendix A,

$$\left[\frac{\partial\phi^*}{\partial\zeta}\right]_-^+ = 0 \quad ; \quad x\in[x_L,\infty)\,.\tag{B-2}$$

The last term in Equation (B-1) vanishes. Infinitely upstream there is no disturbance so that

$$\lim_{R\to\infty}\int_{-H}^{H}\left(\phi^*\cdot\frac{\partial\psi}{\partial\xi}-\psi\cdot\frac{\partial\phi^*}{\partial\xi}\right)\Big|_{\xi=-R}d\xi = 0\,.\tag{B-3}$$

From Equation (47) it follows

$$\left|\frac{\partial\psi}{\partial\xi}\Big|_{\xi=R}\right| = O\left(\frac{1}{\sqrt{R}}\right) \quad ; \quad [R\to\infty]\,,\tag{B-4}$$

where 'O' is the Landau's symbol in Equation (B-4) and

$$\lim_{R\to\infty}\sqrt{R}\cdot\left|\frac{\partial\psi}{\partial\xi}\Big|_{\xi=R}\right| = c\,,\tag{B-5}$$

where c is a constant number. Similarly

$$|\psi|_{\xi=R}| = O\left(\frac{1}{\sqrt{R}}\right) \quad ; \quad [R\to\infty]\,.\tag{B-6}$$

Let

$$|\phi^*|_{\xi=R}| = o(\sqrt{R}) \quad ; \quad [R\to\infty]\,,\tag{B-7}$$

and

$$\left|\frac{\partial\phi^*}{\partial\xi}\Big|_{\xi=R}\right| = o(\sqrt{R}) \quad ; \quad [R\to\infty]\,,\tag{B-8}$$

where 'O' is also the Landau's symbol and Equation (B-7) becomes

$$\lim_{R\to\infty} \frac{|\phi^*|_{\xi=R}|}{\sqrt{R}} = 0 \ . \tag{B-9}$$

Then

$$\left| \int_{-H}^{H} \left(\phi^* \cdot \frac{\partial \psi}{\partial \xi} - \psi \cdot \frac{\partial \phi^*}{\partial \xi} \right)\Big|_{\xi=R} d\zeta \right| \to 0 \quad ; \quad R \to \infty \ . \tag{B-10}$$

Experimentally, the conditions (B-7) and (B-8) are always satisfied except for the case of tunnel resonance. Equation (B-1) then becomes Equation (51).

REPORT DOCUMENTATION PAGE / PAGE DE DOCUMENTATION DE RAPPORT

REPORT/RAPPORT 1a	REPORT/RAPPORT 1b
NAE-AN-9	NRC No. 21274
REPORT SECURITY CLASSIFICATION / CLASSIFICATION DE SÉCURITÉ DE RAPPORT 2	**DISTRIBUTION (LIMITATIONS) 3**
Unclassified	Unlimited

TITLE/SUBTITLE/TITRE/SOUS-TITRE 4

A New Method of Estimating Wind Tunnel Wall Interference in the Unsteady Two-Dimensional Flow

AUTHOR(S)/AUTEUR(S) 5

H. Sawada, visiting scientist
2nd Aerodynamics Division, National Aerospace Laboratory, Japan

SERIES/SÉRIE 6

Aeronautical Note

CORPORATE AUTHOR/PERFORMING AGENCY/AUTEUR D'ENTREPRISE/AGENCE D'EXÉCUTION 7

National Research Council Canada
National Aeronautical Establishment High Speed Aerodynamics Laboratory

SPONSORING AGENCY/AGENCE DE SUBVENTION 8

DATE 9	FILE/DOSSIER 10	LAB. ORDER / COMMANDE DU LAB. 11	PAGES 12a	FIGS/DIAGRAMMES 12b
83-01			60	29

NOTES 13

DESCRIPTORS (KEY WORDS)/MOTS-CLÉS 14

1. Wind tunnel interference
2. Unsteady flow

SUMMARY/SOMMAIRE 15

A new method of estimating wall interference in unsteady flow is presented. This method is valid for subcritical flow within the accuracy of the linearized small disturbance theory. The main feature of the method is the use of measured pressure along lines in the flow direction near the tunnel walls. This method is particularly effective in a tunnel with ventilated walls because it does not require the representation of wall characteristics with unreliable mathematical expressions. Results of some numerical examples indicate that the new method produces satisfactory results except for cases when the reduced frequencies are close to the tunnel resonance frequencies. For the case of an airfoil in pitching motion, the method has been used to correct the amplitude of the angle of attack and the time lag in the motion.